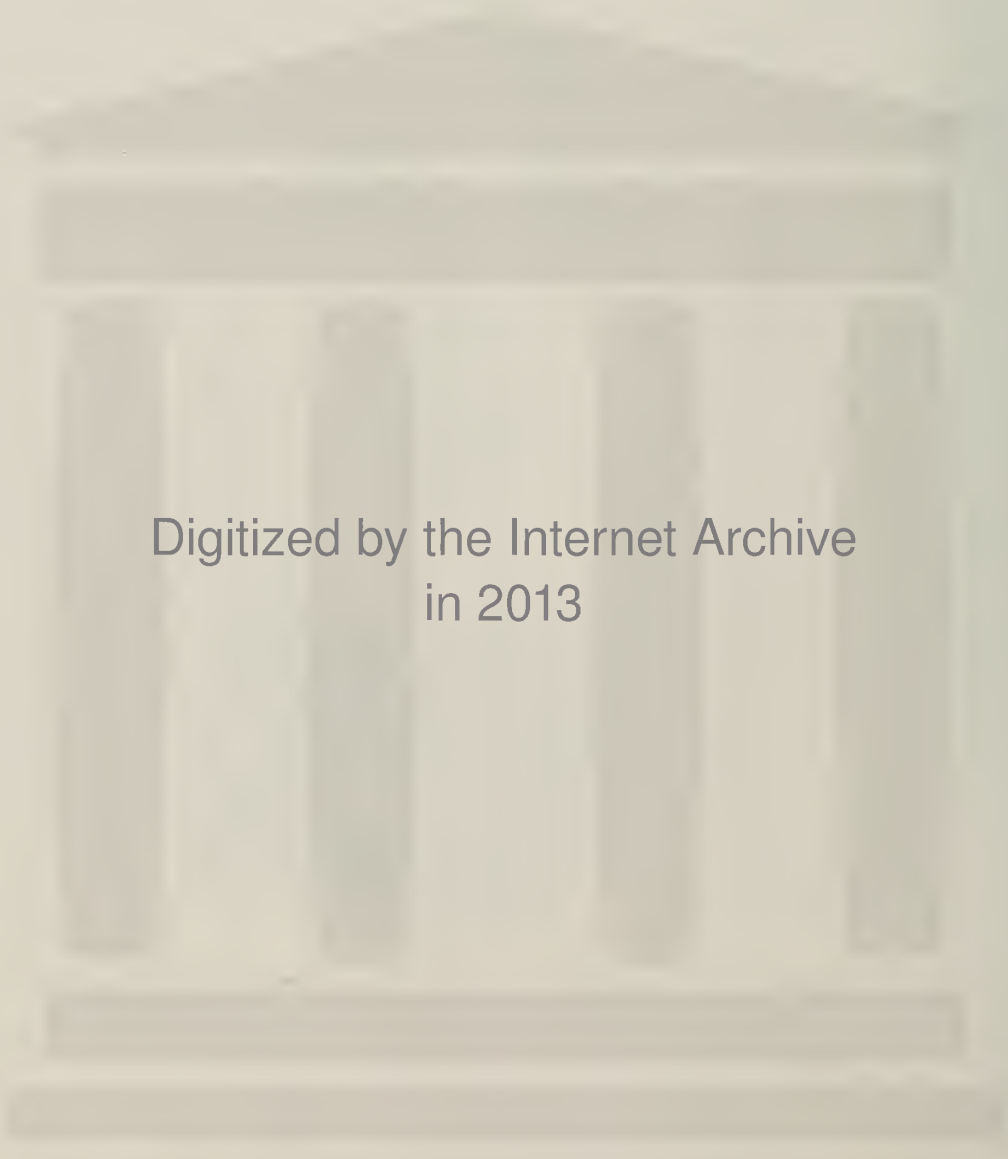

UIUCDCS-R-75-723

MOLECULAR STOCHASTICS: A STUDY OF DIRECT PRODUCTION OF STOCHASTIC SEQUENCES FROM TRANSDUCERS

by

James Roland Cutler

April, 1975

DEPARTMENT OF COMPUTER SCIENCE
UNIVERSITY OF ILLINOIS AT URBANA-CHAMPAIGN · URBANA, ILLINOIS

UIUCDCS-R-75-723

MOLECULAR STOCHASTICS: A STUDY OF DIRECT PRODUCTION OF STOCHASTIC SEQUENCES FROM TRANSDUCERS

BY

JAMES ROLAND CUTLER

April 1975

Department of Computer Science
University of Illinois
Urbana, Illinois 61801

This work was supported in part by Contract No. N000-14-67-A-0305-0024 and was submitted in partial fulfillment of the requirements for the degree of Doctor of Philosophy in Computer Science, at the University of Illinois.

MOLECULAR STOCHASTICS: A STUDY OF DIRECT PRODUCTION OF STOCHASTIC SEQUENCES FROM TRANSDUCERS

James Roland Cutler
Department of Computer Science
University of Illinois at Urbana-Champaign, 1975

ABSTRACT

Molecular Stochastics is an extension of stochastic computing. The main concern of Molecular Stochastics is the generation of stochastic sequences that are used as the encoded information in stochastic computing. Also, these stochastic sequences in order to have meaning should be dependent upon some physical parameter of interest such as temperature. Thus, the problem is constructing a transducer which outputs a stochastic sequence that varies with respect to a physical parameter.

This paper presents the necessary theory along with a discussion of a number of noise sources. These sections imply a number of transducers which were constructed and tested. The data was then compared with the result predicted by the theory.

ACKNOWLEDGMENT

The author wishes to express his gratitude to his advisor, Professor W. J. Poppelbaum, for his ideas, assistance and friendship on this project.

He is indebted to Frank Serio, Sam McDowell, and Bill Marlatt who did exceptional work on the fabrication and assembly of the stochastic meter. He also wishes to acknowledge Stanley Zundo for the drawings, Dennis Reed for the printing and Evelyn Huxhold for her excellent work in typing the manuscript. Also, he thanks the members of the Information Engineering Laboratory for their enlightening discussions.

He especially thanks his wife, Joyce, for her help in proofreading and for her encouragement.

TABLE OF CONTENTS

LIST OF FIGURES

Figure Page

LIST OF TABLES

LIST OF SYMBOLS

$f_X(x)$ - first order density function of the stationary random process, $X(t)$

$P(\varepsilon)$ - probability of the event, ε, occurring

$F_X(x)$ - first order distribution function of $X(t)$

$f_X(x_1, x_2; \tau)$ - second order density function of $X(t)$

$F_X(x_1, x_2; \tau)$ - second order distribution function of $X(t)$

$\Phi_X(\omega) = \int_{-\infty}^{\infty} f_X(x)\, e^{-j\omega x}\, dx$ - characteristic function of $X(t)$

$\Psi_X(\omega) = \ln\, \Phi_X(\omega)$

$\mu_X = E\{(X(t)\}$ - expected value (mean) of $X(t)$

[by definition, $\mu_X = \int_{-\infty}^{\infty} x\, f_X(x)\, dx$]

$\sigma_X^2 = E\{ (X(t) - \mu_X)^2\}$ - variance of $X(t)$

[by definition, $\sigma_X^2 = \int_{-\infty}^{\infty} (x - \mu_X)^2\, f_X(x)\, dx$ and σ_X is called the standard deviation of $X(t)$]

$R_X(\tau) = E\{ X(t + \tau)\, X(t)\}$ - autocorrelation function of $X(t)$

$S_X(\omega) = \int_{-\infty}^{\infty} R_X(\tau)\, e^{-j\omega\tau}\, d\tau$ - power spectrum of $X(t)$

1. INTRODUCTION

Molecular Stochastics as defined by Poppelbaum[1] is the study of the statistical parameters of the random fluctuations on a molecular level, and the use of these parameters (averages, variance) to assess physical parameters like temperature, pressure, velocity, etc. The methods of stochastic processing are used throughout[2, 3, 4, 5] and we shall begin by summarizing these methods.

To encode information in stochastic processing, a number is represented as the probability of appearance of a 1 in a given time slot in a sequence of time slots. The multiplication of two numbers is very simple: The use of an AND gate is sufficient. Thus, the beauty of stochastic processing is that the arithmetic unit is very simple and an approximation to the result is available immediately: The accuracy of the result is, of course, determined by the length of the sample period. Certain generalizations of this so-called synchronous random pulse sequence (SRPS) system are sometimes useful, for instance one can take away the condition of the pulses occuring at fixed times.

In previous research it has been shown that the results of very complicated formulas may be found quickly and easily by stochastic computing. An example of this, which has actually been implemented, is the On-line Fourier Transform of a 32 x 32 input matrix. The calculations are done by 1024 separate stochastic arithmetic units: Because the arithmetic units of a stochastic computer are so simple (and small), the cost (in terms of both space and money) of such a large number of arithmetic units is not prohibitive!

Up to now, the emphasis in stochastics has been placed on the computation using the stochastic sequences, and not upon the production of the sequences: The stochastic sequences were conversions of digital or analog data.

In Molecular Stochastics we aim at the direct production of stochastic sequences from transducers. The basic premise in Molecular Stochastics is that the physical variables in our environment (such as temperature) have a random component, and that this random component expresses somehow the physical variables under consideration. The random component may occur naturally (i.e., it was present before the measurement) or may occur artificially (i.e., it is present in the measuring instrument). Usually this component is filtered out or averaged so that the result is either an analog measurement or a digital measurement. This study will use the random component to produce the measurement.

2. GENERAL THEORY

Calculations that follow in section 2.1 show that if the random component depends upon the physical variable, the stochastic sequence engendered by the random component will be useful to measure this variable. In particular the mean, variance, and autocorrelation function of the stochastic sequence will depend on the variable and can thus be used as a measure of the physical phenomenom.

Section 2.2 contains a discussion of the necessary conditions for the property of ergodicity. Ergodicity occurs when the mean of the stochastic sequence is equal to the time average of the stochastic sequence. Thus, if the property of ergodicity is present, the mean of the sequence can be measured by finding the time average.

A finite time average is used to approximate the mean of the stochastic sequence. Section 2.3 discusses the errors produced and methods which can be used to minimize errors.

2.1 Calculation of the Mean of the Stochastic Sequence

First, a general model of a transducer is needed. Figure 2.1 shows the block diagram of a transducer which can produce a stochastic sequence from a random process. Figure 2.2 shows a typical input and its corresponding output.

Let us find the condition necessary for the stochastic sequence $Y(t)$ to be dependent upon the measurement. Calculating the mean and variance of $Y(t)$ (in Figure 2.1) is straightforward given the density of $X(t)$.

$$Y(t) = \begin{cases} 1 & \text{if } X(t) \geq A \\ 0 & \text{otherwise} \end{cases}$$

Then,
$$\mu_Y = P[Y(t) = 1] = P[X(t) \geq A]$$

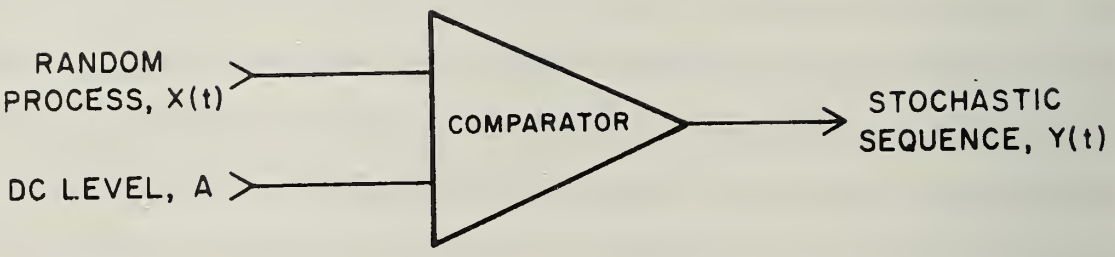

Figure 2.1 Block Diagram of a Transducer

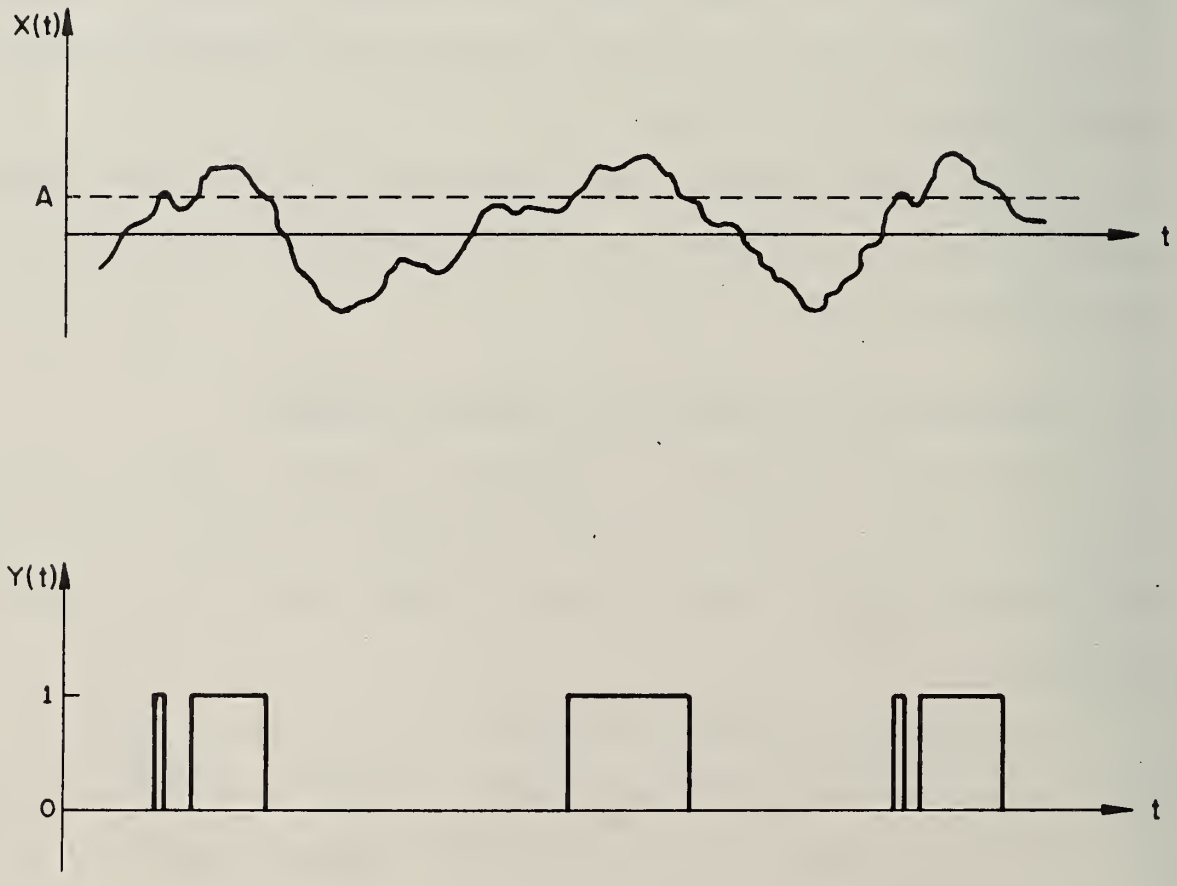

Figure 2.2 Typical Input X(t) and Corresponding Output Y(t)

or $$\boxed{\mu_Y = 1 - F_X(A)}$$

And, $$\sigma_Y^2 = E[Y^2(t)] - \mu_Y^2$$

But, $$E[Y^2(t)] = P[Y(t) = 1] = \mu_Y$$

$$\boxed{\sigma_Y^2 = \mu_Y(1 - \mu_Y)}$$

It is obvious that $0 \leq \mu_Y \leq 1$, and $0 \leq \sigma_Y^2 \leq 1/4$. Also, in order for the mean of $Y(t)$ to depend upon the variable, the density of $X(t)$ must depend upon that variable. In most cases, if either μ_X of σ_X^2 have a dependence upon the variable, μ_Y depends upon the variable to be measured. For example, suppose that $X(t)$ is Gaussian distributed with mean μ_X and variance σ_X^2

[$\Rightarrow f_{X(t)}(x) = \frac{1}{\sigma_X\sqrt{2\pi}} \exp \frac{-(x-\mu_X)^2}{2\sigma_X^2}$], then $\mu_Y = \frac{1}{2} - \text{erf}(\frac{A-\mu_X}{\sigma_X})$. [$\text{erf}(x) = \frac{1}{\sqrt{2\pi}} \int_0^x e^{-\frac{y^2}{2}} dy$]. Note that μ_Y is dependent upon the random process $X(t)$ unless μ_X is a constant equal to A: In that case, $\mu_Y = 1/2$ for all σ_X. Assuming that $\mu_X = 0$, Figure 2.3 shows a graph of μ_Y with respect to σ_X.

Thus it has been shown that in general the mean of the stochastic sequence $Y(t)$ varies as the density of the random process $X(t)$ varies. There are a few cases, however, when the mean does <u>not</u> change even if the density of $X(t)$ varies.

2.2 Ergodicity of X(t)

An ergodic process is one in which the mean and the time average are the same. Before mathematically defining ergodicity and giving an explanation of a necessary condition for ergodicity, we have to introduce the notion of autocorrelation function: It is given by

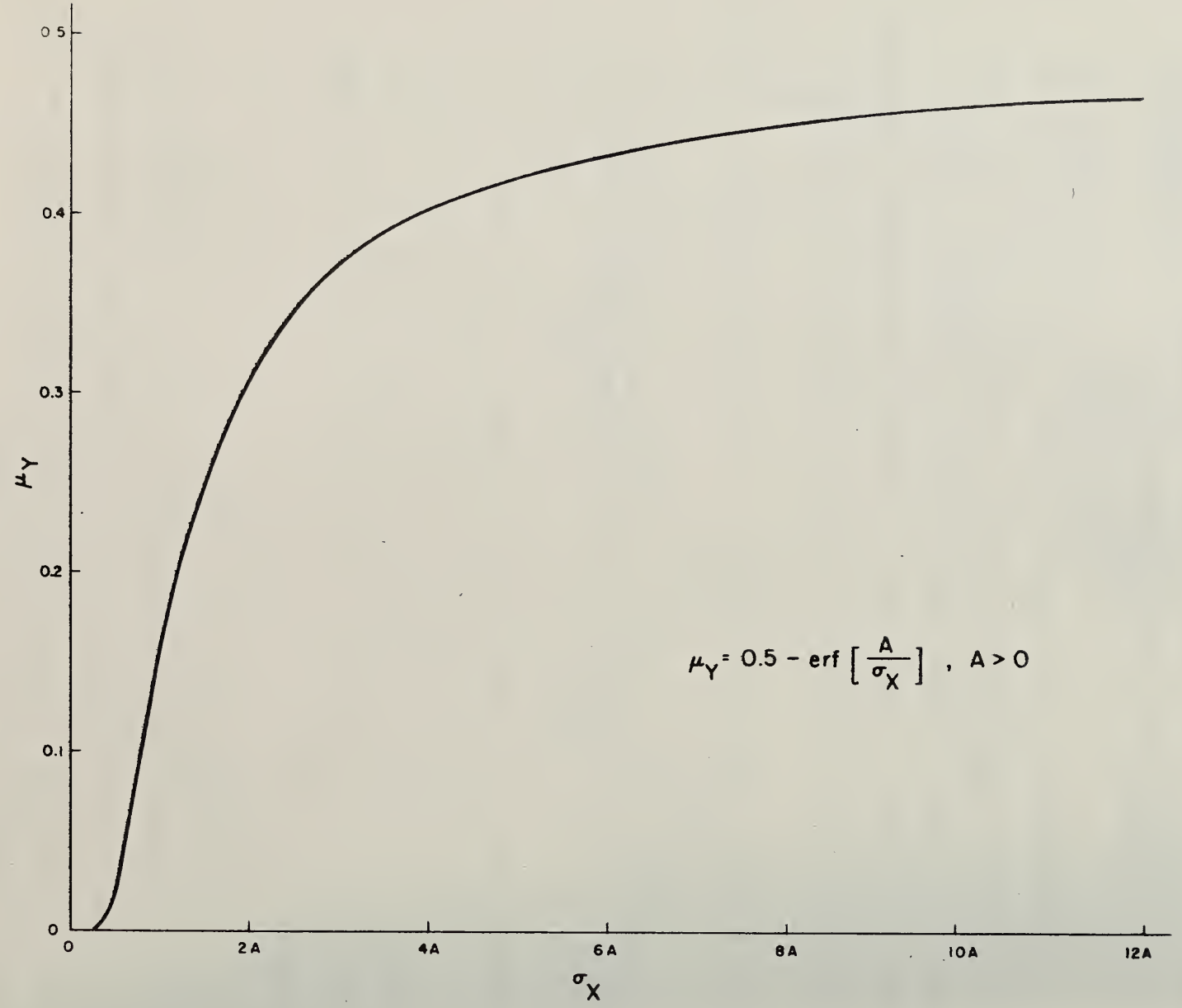

Figure 2.3 μ_Y vs. σ_X

$$R_Y(\tau) = E\{Y(t + \tau)\, Y(t)\}$$

$$= P\{Y(t + \tau) = 1 \text{ and } Y(t) = 1\}$$

$$= P\{X(t + \tau) \geq A \text{ and } X(t) \geq A\}$$

$$= 1 - 2\, F_X(A) + F_X(A, A; \tau)$$

In most cases, it is difficult to calculate the closed form of the autocorrelation function. However, since it is a probability, there are limits that may be put on it; i.e., $0 \leq R_Y(\tau) \leq 1$. In specific cases it is possible to have better limits.

In order to measure the mean of $Y(t)$, the property of ergodicity must be present: The stochastic sequence $Y(t)$ is ergodic if the mean is equal to the time average or, mathematically,

$$\mu_Y = \lim_{T\to\infty} \frac{1}{T} \int_0^T Y(t)dt$$

A theorem allows us to judge the ergodicity of a random process: It states that $\mu_Y = \lim_{T\to\infty} \frac{1}{T} \int_0^T Y(t)dt$ if and only if

$$\lim_{T\to\infty} \frac{2}{T} \int_0^T (1 - \frac{t}{T})(R_Y(t) - \mu_Y{}^2)dt = 0 \qquad \text{(a)}$$

(Note that equation (a) is equivalent to $\lim_{T\to\infty} \frac{1}{T} \int_0^T R(t)dt = \mu_Y{}^2$). Using this theorem, the stochastic sequence $Y(t)$ is ergodic ($\mu_Y = 1 - F_X(A) = \lim_{T\to\infty} \frac{1}{T} \int_0^T Y(t)dt$) if and only if

$$\lim_{T\to\infty} \frac{1}{T} \int_0^T [1 - 2F_X(A) + F_X(A, A; \tau)]d\tau = \mu_Y{}^2 = [1 - F_X(A)]^2$$

which is equivalent to $\lim_{T\to\infty} \frac{1}{T} \int_0^T F_X(A, A; \tau)d\tau = F_X{}^2(A)$. A necessary condition for ergodicity (but not a sufficient condition) is that $\lim_{T\to\infty} R(\tau) = \mu_Y{}^2$ or $\lim_{T\to\infty} F_X(A, A; \tau) = F_X{}^2(A)$, which implies that $X(t + \tau)$ and $X(t)$ are uncorrelated as $\tau\to\infty$.

2.3 Determination and Errors of a Finite Time Average

There is one more important consideration that must be presented; i.e., the determination of the time average. As explained in later sections, the method that is used is the sampling of the stochastic sequence $Y(t)$. Suppose that Y_k is defined as follows:

$$Y_k = \begin{cases} 1 \text{ if } Y(k\lambda) = 1 \\ 0 \text{ if } Y(k\lambda) = 0 \end{cases} \qquad \text{where } \lambda \text{ is the sampling period}$$

Y_k is now the sampled version of $Y(t)$. Figure 2.4 shows a typical stochastic sequence $Y(t)$ and the corresponding Y_k.

The problem now is to determine λ and the a_k's so that

$$\frac{1}{N\lambda} \int_0^{N\lambda} Y(t)dt \sim \sum_{k=1}^{N} a_k Y_k$$

There are several criteria that may be used to determine the unknowns. One possibility is to minimize the probability

$$P\{|A(Y) - \hat{A}(Y)| > C\}$$

where $A(Y) = \frac{1}{N\lambda} \int_0^{N\lambda} Y(t)dt$ and $\hat{A}(Y) = \sum_{k=1}^{N} a_k Y_k$. This is in many cases very difficult to accomplish since the density of the error, $|A(Y) - \hat{A}(Y)|$, would have to be determined. A more reasonable solution is the minimizing of the mean-square error, e.

$$e = E\{|A(Y) - \hat{A}(Y)|^2\}$$

A theorem states that the mean-square error is minimized if

$$E\{[A(Y) - \hat{A}(Y)]\, Y_k\} = 0 \quad \text{for } k = 1, 2, \ldots, N \qquad (b)$$

(i.e., the samples, Y_k, are orthogonal to the error) and the minimum error, e_m, is $e_m = E\{[A(Y) - \hat{A}(Y)]\, A(Y)\}$. Making the appropriate substitutions, the equation (b) may be written

$$\frac{1}{N\lambda} \int_0^{N\lambda} R(t - n\lambda)\, dt = \sum_{k=1}^{N} a_k R[(k - n)\lambda] \quad \text{for } n = 1, 2, \ldots, N$$

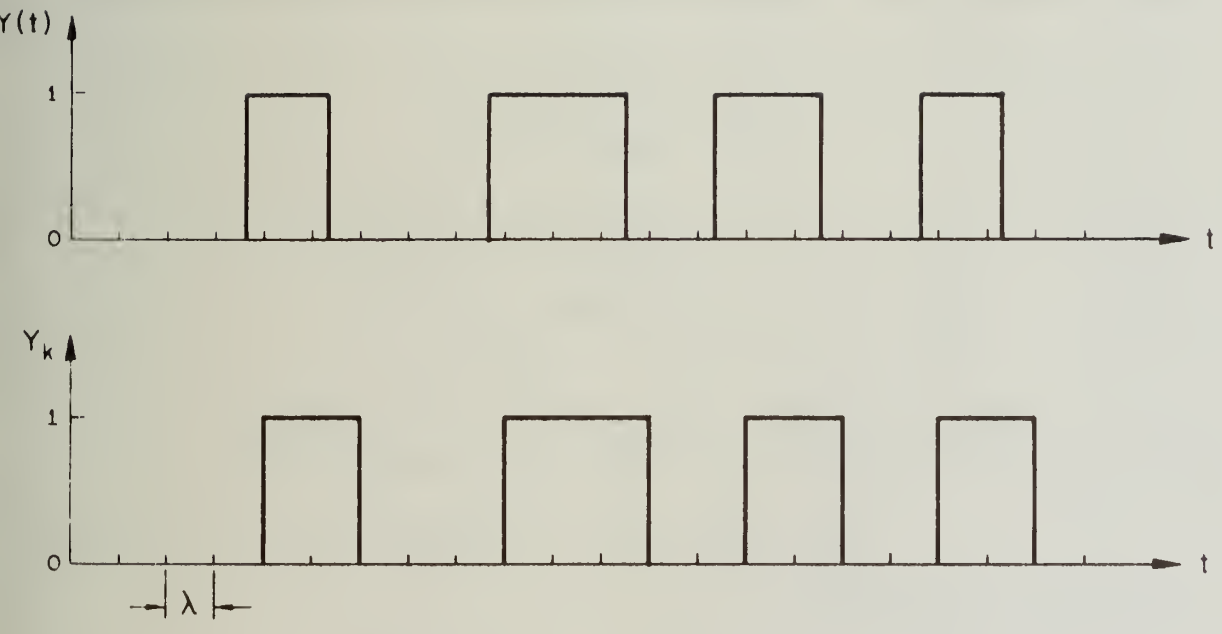

Figure 2.4 Example of Y(t) and the Corresponding Y_k

For a given $R(\tau)$ and a desired sampling rate, λ, solutions may be found for the a_k's since there are N unknowns and N linear equations. The minimum mean-square error is

$$e_m = \frac{1}{N\lambda}\int_0^{N\lambda}\left(1 - \frac{t}{N\lambda}\right) R(t)dt \; - \; \frac{1}{N\lambda}\int_0^{N\lambda}\sum_{k=1}^{N} a_k \, R(t - k\lambda)dt$$

In considering the value of the sampling rate, it is obvious that the smaller λ becomes, the smaller the error, e_m, becomes. However, there is one other observation that may be made about the sampling rate, λ. If λ is selected such that $R(t+\lambda) \simeq R(t)$ for any t, the integral and the summation of $R(t)$ are approximately the same. (It is assumed that $R(t)$ is continuous). Suppose that

$$\left|\int_0^{N\lambda} R(t)dt - \lambda \sum_{k=0}^{N-1} R(k\lambda)\right| \leq \varepsilon$$

is to be satisfied for some $\varepsilon > 0$ by choosing an appropriate λ:

$$\lambda \sum_{k=0}^{N-1} R(k\lambda) - \varepsilon \leq \int_0^{N\lambda} R(t)dt \leq \lambda \sum_{k=0}^{N-1} R(k\lambda) + \varepsilon$$

But, $$\int_0^{N\lambda} R(t)dt = \int_0^{\lambda} R(t)dt + \int_{\lambda}^{2\lambda} R(t)dt + \ldots + \int_{(N-1)\lambda}^{N\lambda} R(t)dt$$

$$= R(t_0) + \lambda R(t_1) + \ldots + \lambda R(t_{N-1}) \quad \text{where} \quad k\lambda \leq t_k \leq (k+1)\lambda$$

since $R(t)$ is continuous.

So, $$\lambda \sum_{k=0}^{N-1} R(k\lambda) - \varepsilon \leq \lambda \sum_{k=0}^{N-1} R(t_k) \leq \lambda \sum_{k=0}^{N-1} R(k\lambda) + \varepsilon$$

$$\sum_{k=0}^{N-1} \left[R(k\lambda) - \frac{\varepsilon}{N\lambda}\right] \leq \sum_{k=0}^{N-1} R(t_k) \leq \sum_{k=0}^{N-1} \left[R(k\lambda) + \frac{\varepsilon}{N\lambda}\right]$$

Thus, if $$\left|R(t_k) - R(k\lambda)\right| \leq \frac{\varepsilon}{N\lambda}$$

then $$\left|\int_0^{N\lambda} R(t)dt - \lambda \sum_{k=0}^{N-1} R(k\lambda)\right| \leq \varepsilon$$

A stronger condition is

$$|R(t + \lambda) - R(t)| \leq \frac{\varepsilon}{N\lambda}$$

for any t. Note that if $R(\lambda) \tilde{=} R(0)$, the probability of the stochastic sequence changing in the interval $(t, t + \lambda)$ is very small. By the Tchebycheff inequality,

$$P\{|Y(t + \lambda) - Y(t)| > \eta\} < \frac{\varepsilon}{N\lambda\eta^2}$$

In summary, a concept of sampling Y(t) was introduced and this sample, Y_k, was used to approximated the time average of Y(t). An error calculation was then made using the mean-square value of the difference, $A(Y) - \hat{A}(Y)$, as the error. This discussion will be referred to in section 5.1.

3. NOISE SOURCES

In this section we shall give a discussion of the types of noise sources which may be used to construct transducers. There are two methods by which a noise source may be obtained: 1) electronic noise such as thermal or shot noise that depend upon the physical parameter of interest or 2) the measurement of a naturally random physical parameter such as turbulent flow.

These noise sources will provide the random process input to the comparator (as in Figure 2.1).

3.1 Thermal Noise

This noise is common and well-known. It is caused by the random movement of thermally excited electrons in a conductor. It has been shown theoretically and experimentally that the voltage power spectrum, S_v, of the thermal noise of a conductor is:

$S_v = 2kTR$ where k = Boltzmann's constant
T = absolute temperature
R = resistance of the conductor.

Using this equation, the rms noise voltage, E_t ($E_t^2 = 2S_v \Delta f$ where Δf = noise bandwidth), is 4 nv. for a 1000Ω resistor and a bandwidth of 1 Hz and is 40 μv. for a 100 K resistor and a bandwidth of 1 MHz. Thus, for a reasonable size resistance and bandwidth, the rms noise is quite low (< 1 mv.) and amplification will be necessary. Figure 3.1 shows the proper modification of Figure 2.1 to obtain a stochastic sequence.

Thermal noise is generally assumed to be Gaussian distributed with zero mean and the power spectrum as above. Suppose that the transfer function, $H(j\omega)$, of the amplifier is:

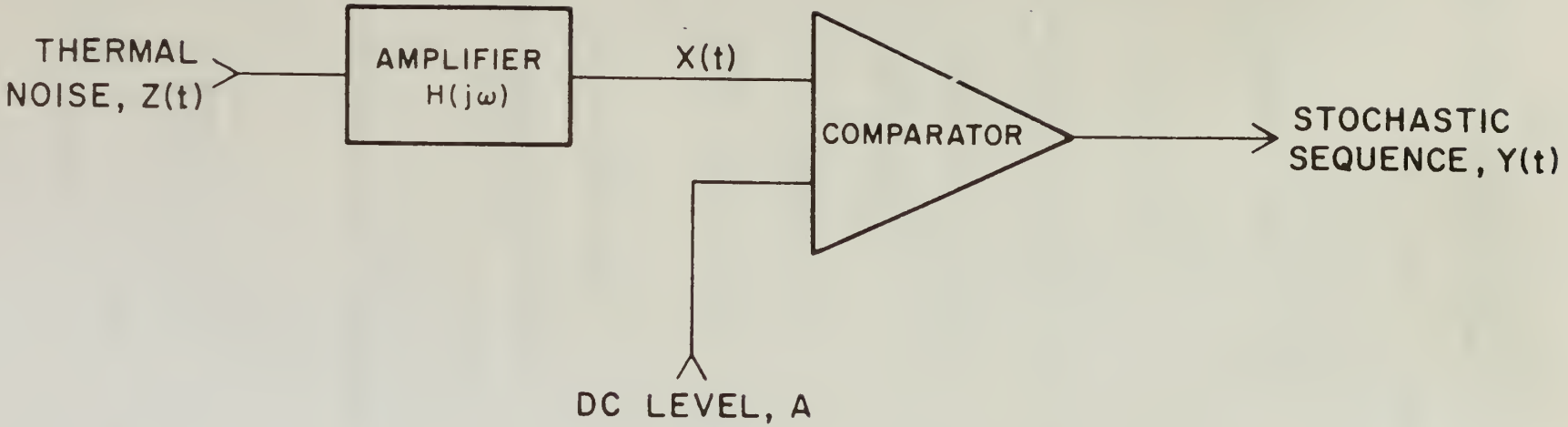

3.1 Block Diagram of the Temperature Transducer

$$H(j\omega) = \frac{G\sqrt{2\alpha}}{j\omega + \alpha}$$

This implies that the amplifier is a low pass filter with gain, G and a corner frequency of $\frac{\alpha}{2\pi}$.

The random process, X(t), is still Gaussian. The mean, μ_X, is:

$$\mu_X = \int_{-\infty}^{\infty} E\{Z(t - \alpha)\}\, h(\alpha)\, d\alpha$$

$$= H(0)\, \mu_Z$$

$$= 0$$

The autocorrelation, $R_X(\tau)$, and power spectrum, $S_X(\omega)$, are:

$$S_X(\omega) = |H(j\omega)|^2\, S_Z(\omega)$$

$$= \frac{2\alpha\, G^2}{\omega^2 + \alpha^2}\, (2kTR)$$

and $$R_X(\tau) = 2kTR\, G^2\, e^{-\alpha|\tau|}$$

Note that $$R_X(0) = \sigma_X^{\,2} = 2kTR\, G^2$$

As shown earlier,

$$\mu_Y = P\{X(t) \geq A\}$$

$$= \frac{1}{2} - \mathrm{erf}\left(\frac{A}{\sigma_X}\right) \quad \text{where} \quad \sigma_X = G\sqrt{2kTR}$$

and,

$$R_Y(\tau) = P\{X(t) \geq A \text{ and } X(t + \tau) \geq A\}$$

$$= \int_A^{\infty}\int_A^{\infty} \frac{1}{2\pi\, \sigma_X^2 \sqrt{1 - r^2}}\, e^{-\frac{(x_1^{\,2} - 2rx_1x_2 + x_2^{\,2})}{2\sigma_X^{\,2}(1 - r^2)}}\, dx_1\, dx_2$$

where $$r = e^{-\alpha|\tau|}$$

$$= \left[\frac{1}{2} - \operatorname{erf}\left(\frac{A}{\sigma_X}\right)\right]^2 + \int_0^r \frac{1}{2\pi\sqrt{1 - z^2}} e^{-\frac{A^2}{(1 + z)\sigma_X^2}} dz$$

From this expression, it is obvious that Y(t) is ergodic.

$$C_Y(\tau) = \int_0^r \frac{1}{2\pi\sqrt{1 - z^2}} e^{-\frac{A^2}{(1 + z)\sigma_X^2}} dz$$

which implies that $\frac{\sin^{-1} r}{2\pi} e^{-\frac{A^2}{(1 + r)\sigma_X^2}} \leq \frac{1}{T}\int_0^T C_Y(\tau) \leq \frac{\sin^{-1} r}{2\pi} e^{-\frac{A^2}{\sigma_X^2}}$

As $T \to \infty$, both sides of the inequality approach zero. Thus, Y(t) is ergodic. It is obvious that $0 \leq \mu_Y \leq 1$ and that $\left[\frac{1}{2} - \operatorname{erf}\left(\frac{A}{\sigma_X}\right)\right]^2 \leq R_Y(\tau) - \frac{1}{2} - \operatorname{erf}\left(\frac{A}{\sigma_X}\right)$. Also, $R_Y(\tau)$ is a continuous function and monotonically decreasing as $|\tau|$ increases.

It may be shown that the slope of $R_Y(\tau)$ is a maximum at $\tau = 0$. So in order to satisfy the condition $R(t + \lambda) - R(t) \leq \frac{\varepsilon}{N\lambda}$ from section 2.3, it is sufficient to satisfy

$$|R(\lambda) - R(0)| \leq \frac{\varepsilon}{N\lambda}$$

From these equations, it is possible to determine the minimum sampling rate given the characteristics of the amplifier, the sampling period and the maximum error for the time average. These results are used in Section 5.2.

This discussion may be repeated for a bandpass or a high pass amplifier. The only change in the results will be in the correlation coefficient, $r(\tau)$. This change will only affect the calculation of the sampling period since the maximum slope of $R_Y(\tau)$ may no longer be at the origin.

The sensitivity of the mean of the stochastic sequence with respect to the temperature and the variable, A, is an important parameter.

Sensitivity is the slope of the function, μ_Y, with respect to temperature. Suppose that a temperature range of $T_1 \leq T \leq T_2$ is to be considered and

$$\Delta = \mu_Y(T_2, A) - \mu_Y(T_1, A)$$

Then

$$\frac{d\Delta}{dA} = \frac{1}{K\sqrt{T_2}} e^{-\frac{A^2}{2K^2T_2}} - \frac{1}{K\sqrt{T_1}} e^{-\frac{A^2}{2K^2T_1}}$$

Setting the derivative equal to zero yields

$$A = K\sqrt{\frac{T_1 T_2}{T_2 - T_1}(\ln T_2 - \ln T_1)}$$

where T_1, T_2 are in °K. Figure 3.2 shows the variation of μ_Y with respect to temperature. The temperature range is -40°C to 100°C and according to the calculations above the greatest deviation in μ_Y will occur when A = 17K. One observation of this graph is that the change of μ_Y is small (< 0.05) even at the optimum setting of A.

3.2 Shot Noise

Shot noise is caused by the random emission of electrons or the random passage of electrons across potential barriers. It is common in diodes or other similar devices. It is experimentally known that shot noise has a power spectrum, $S_I(\omega)$, of

$$S_I(\omega) = qI \quad \text{where} \quad q = \text{electron charge}$$

$$I = \text{current flowing in the diode.}$$

Since $q = 1.59 \times 10^{-19}$ coulombs, the power spectrum and, as a consequence, the rms noise current are small values (~ 1 pa for I = 1 μa and Δf = 1 Hz). However, in certain devices there is an internal mechanism which multiplies this noise. A discussion of this multiplication will come in Section 4.1.

Shot noise is generally modelled as a summation of pulses

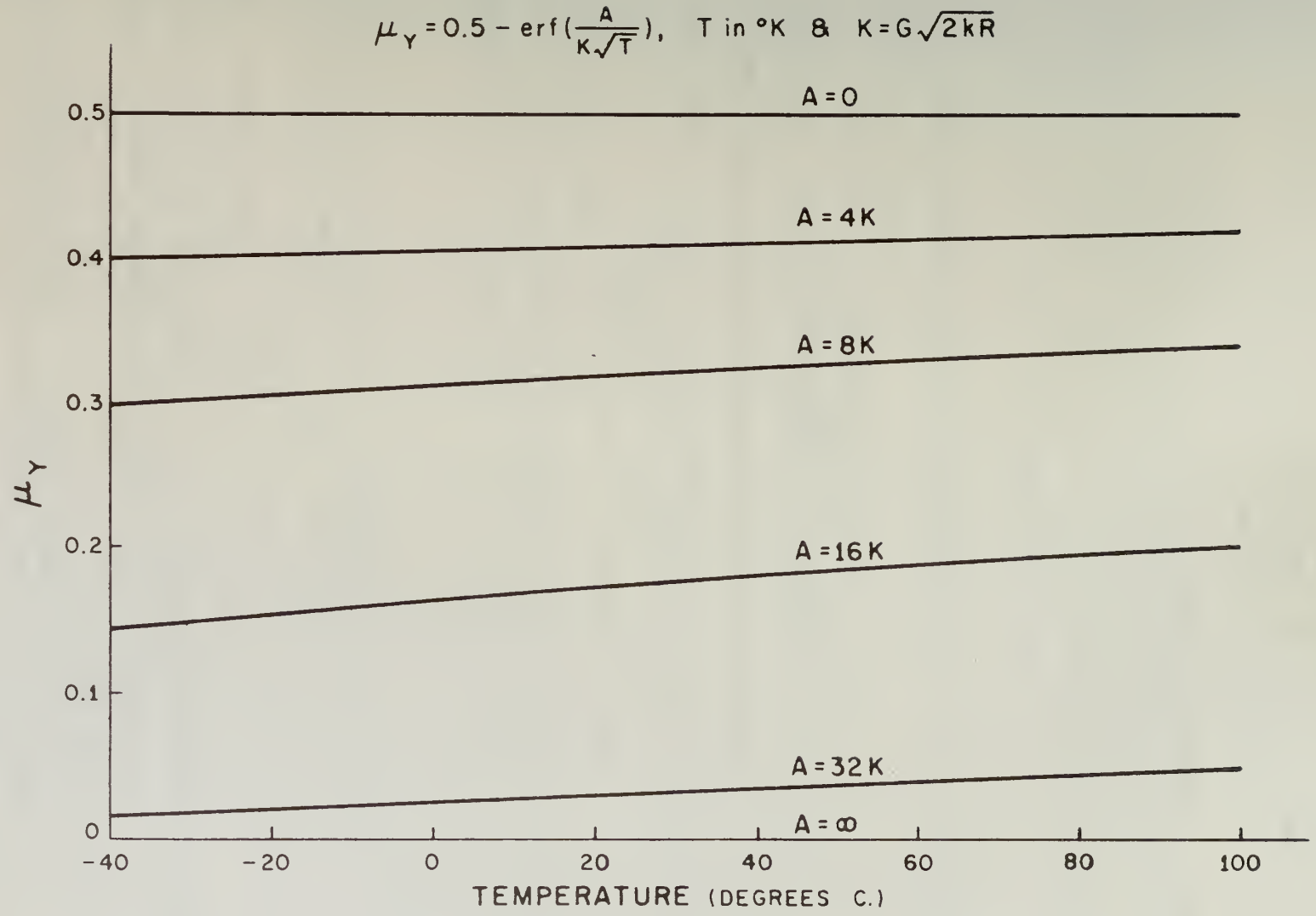

Figure 3.2 μ_Y vs. Temperature

$$I(t) = \sum_i h(t - t_i)$$

where $h(\tau)$ may have any shape (in this discussion, it is assumed that $h(\tau)$ is triangular), and t_i are random variables that are exponentially distributed with parameter, ρ. Note that $\int_{-\infty}^{\infty} h(t)dt = q$ and that ρ is the average number of electrons transferred per unit time. The power spectrum of $I(t)$ is identical to the power spectrum referred to in the first paragraph, assuming that the triangular pulse is very small. For $I(t) = \sum_i h(t - t_i)$,

$$E\{I(t)\} = \rho q$$

$$R(\tau) = \rho^2 q^2 + \rho \int_{-\infty}^{\infty} h(t)\, h(\tau + t)dt$$

and

$$S(\omega) = 2\pi \rho^2 H(0)\, \delta(\omega) + \rho |H(j\omega)|^2$$

The density of shot noise is difficult to calculate in many cases (i.e., $h(\tau)$ does not have a finite duration). It can be shown that if $h(\tau)$ is a triangular pulse with finite duration, T, the density of $I(t)$ is

$$f(x) = e^{-\rho T}[g_0(x) + \ldots + g_k(x) \frac{(\rho T)^k}{k!} + \ldots]$$

where $g_0(x) = \delta(x)$ and $g_k(x)$ = density of $I(t)$ given that there are k t_i's that occur in the interval $(t - T, k)$. Also, since the t_i's are independent of each other,

$$g(x) = g_1(x)$$

$$g_2(x) = g(x) * g(x) \qquad [* \text{ means convolution}].$$

$$\vdots$$

$$g_k(x) = g(x) * \ldots * g(x) \quad [k \text{ convolutions of } g(x)].$$

There are several interesting points to be made about the above density:

1. As k increases, $g_k(x)$ approaches a Gaussian density. (Central-Limit Theorem).
2. If $\rho T << 1$, $f(x)$ may be approximated by using the first several terms of the sum, i.e.,

$$f(x) \simeq e^{-\rho T}\{g_0(x) + \rho T\, g(x) + \frac{(\rho T)^2}{2}\,[g(x) * g(x)]\}$$

3. If $T \gg 1$, $f(x)$ may be approximated by a Gaussian density.

4. If $T \sim 1$, $f(x)$ is best approximated by adding terms to the sum in comment 2.

It is interesting to note that the characteristic function may be determined if $h(\tau)$ does not have a finite period. In this case.

$$\Psi(\omega) = \rho \int_{-\infty}^{\infty} [e^{j\omega h(t)} - 1]\, dt$$

It is obvious that this equation is very difficult to solve. For example, if $h(t) = e^{-\alpha t}$ for $t \geq 0$,

$$\Psi(\omega) = \frac{\rho}{\alpha}\left[j\omega + \frac{(j\omega)^2}{2\cdot 2!} + \ldots + \frac{(j\omega)^k}{k\cdot k!} + \ldots\right]$$

As stated before, the autocorrelation function is

$$R(\tau) = \rho^2 q^2 + \rho \int_{-\infty}^{\infty} h(t)\, h(t+\tau)dt$$

which implies that

$$C(\tau) = R(\tau) - E^2\{I(t)\}$$

$$= \rho \int_{-\infty}^{\infty} h(t)\, h(t+\tau)dt$$

The only condition necessary for ergodicity of the mean is that

$$\lim_{T\to\infty} \frac{1}{T} \int_0^T C(\tau)d\tau = 0$$

or

$$\lim_{T\to\infty} \frac{\rho}{T} \int_0^T \int_{-\infty}^{\infty} h(t)\, h(t+\tau)dt\, d\tau = 0$$

It is obvious that since $\int_{-\infty}^{\infty} h(t)dt < \infty$, then

$$\int_{-\infty}^{\infty} h(t)\, h(t+\tau) < \infty \qquad \text{for all } \tau$$

and shot noise is ergodic.

In the case of shot noise, the parameter that will vary with respect to some variable to be measured will be the average number of electrons transferred per unit time, ρ. By looking at previous equations, both the mean and variance of $I(t)$ will vary with respect to ρ. Thus, the density of $I(t)$ will shift drastically and the range of the measurement will be very small. (The sensitivity of the measurement will be very good).

The range can be extended by filtering out the mean of $I(t)$. (This can be done by a capacitor). Suppose that $I_0(t)$ is defined as

$$I_0(t) = I(t) - \mu_I$$

so that

$$\mu_{I_0} = 0$$

and $$R_{I_0}(\tau) = \rho \int_{-\infty}^{\infty} h(t)\, h(t+\tau)dt$$

But this definition of $I_0(t)$ is equivalent to

$$I_0(t) = \sum_i h_0(t - t_i)$$

where

$$\int_{-\infty}^{\infty} h_0(t)dt = 0$$

An interesting case occurs if

$$h_0(t) = \begin{cases} a - \dfrac{2at}{T} & \text{for } 0 \leq t \leq T \\ 0 & \text{otherwise} \end{cases}$$

Figure 3.3 shows the graph of $h_0(t)$ and Figure 3.4 shows the resulting densities, g_0, g_1, g_2, and $g_3(x)$ from the sum

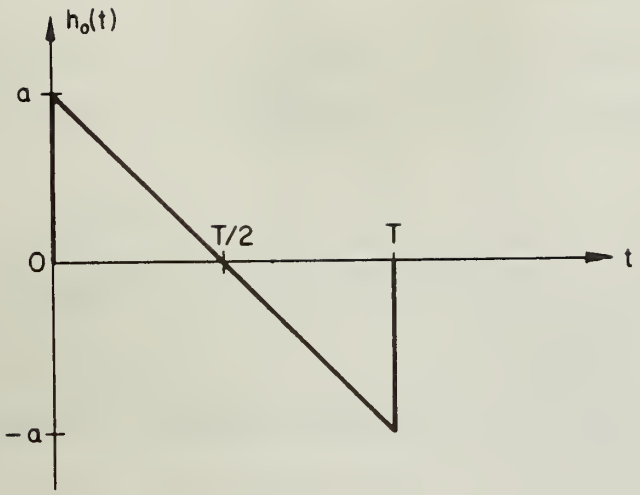

Figure 3.3 Pulse Shape of $h_0(t)$

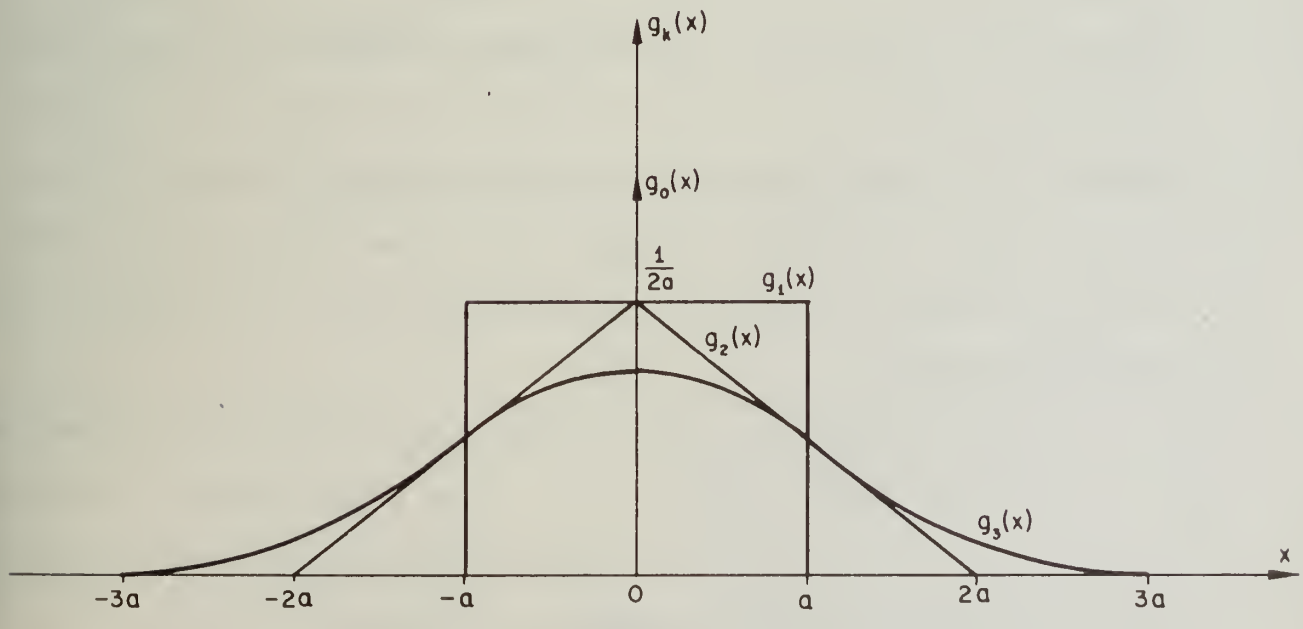

Figure 3.4 Density of $g_0(x)$, $g_1(x)$, $g_2(x)$ and $g_3(x)$

$$f(x) = e^{-\rho T} \left[g_0(x) + \ldots + g_k(x) \frac{(\rho T)^k}{k!} + \ldots \right]$$

As mentioned before, if k is large, $g_k(x)$ may be approximated by a Gaussian density. [The mean of $g_1(x)$ is zero and variance is $\frac{a^2}{3}$].

$$g_k(x) \simeq \frac{1}{a} \sqrt{\frac{3}{2\pi k}} \; e^{-\frac{3x^2}{2k\,a^2}}$$

Figures 3.5, 3.6 and 3.7 show the density of $I_0(t)$ for several values of ρT. Note that the tails of the density expand as ρT becomes larger. Assuming that T is a constant and ρ varies, the density of $I_0(t)$ varies and thus the mean of a stochastic sequence derived from $I_0(t)$ varies.

3.3 Turbulent Flow

There are two types of fluid flow: laminar and turbulent. Turbulent flow occurs if the particles in a fluid have an irregular, fluctuating motion and erratic paths; which in laminar flow, particles have a steady path. Both types of flow obey the laws of fluid dynamics; however, for turbulent flow, the parameters such as pressure and velocity are considered to be random processes. There are two important equations that the parameters of the flow must obey: the equation of conservation of mass and the Navier-Stokes equations of motion. Assuming a constant density fluid, the equation of conservation of mass is

$$\frac{\partial u}{\partial x} + \frac{\partial v}{\partial y} + \frac{\partial w}{\partial z} = 0$$

where u = velocity in the x-direction
v = velocity in the y-direction
and w = velocity in the z-direction

The corresponding Navier-Stokes equations of motion are

$$\rho \frac{\partial u}{\partial t} = - \frac{\partial p}{\partial x} + \frac{\partial}{\partial x} \left(\mu \frac{\partial u}{\partial x} - \rho u^2 \right) + \frac{\partial}{\partial y} \left(\mu \frac{\partial u}{\partial y} - \rho uv \right) + \frac{\partial}{\partial z} \left(\mu \frac{\partial u}{\partial z} - \rho uw \right)$$

$$\rho \frac{\partial v}{\partial t} = - \frac{\partial p}{\partial y} + \frac{\partial}{\partial x} \left(\mu \frac{\partial v}{\partial x} - \rho uv \right) + \frac{\partial}{\partial y} \left(\mu \frac{\partial v}{\partial y} - \rho v^2 \right) + \frac{\partial}{\partial z} \left(\mu \frac{\partial v}{\partial z} - \rho vw \right)$$

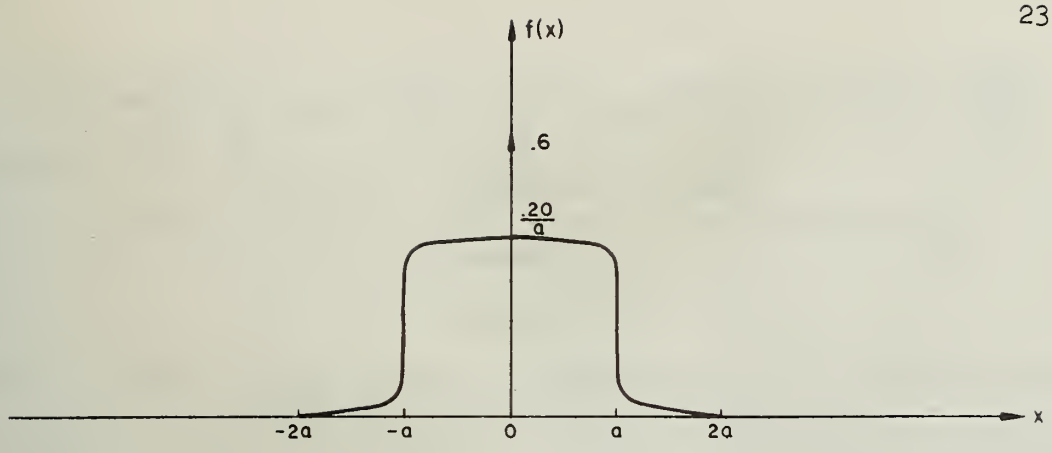

Figure 3.5 Density of $I_0(t)$ for $\rho T = 0.5$

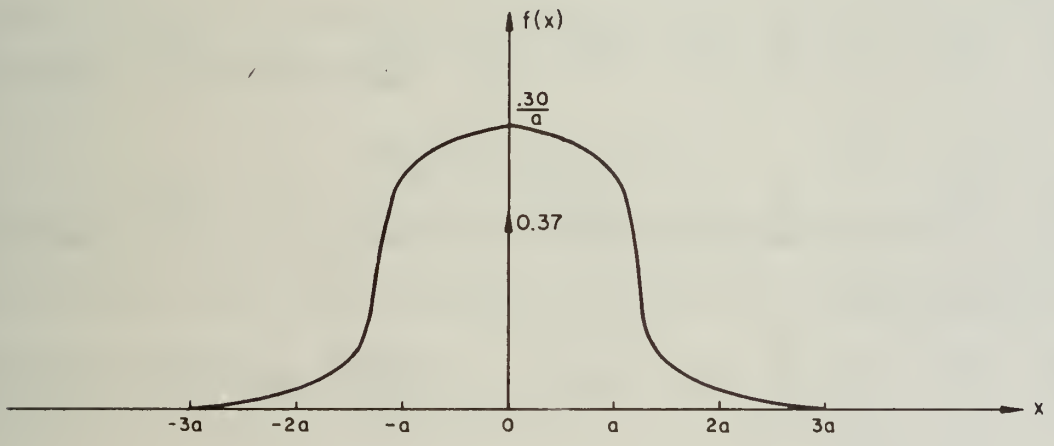

Figure 3.6 Density of $I_0(t)$ for $\rho T = 1.0$

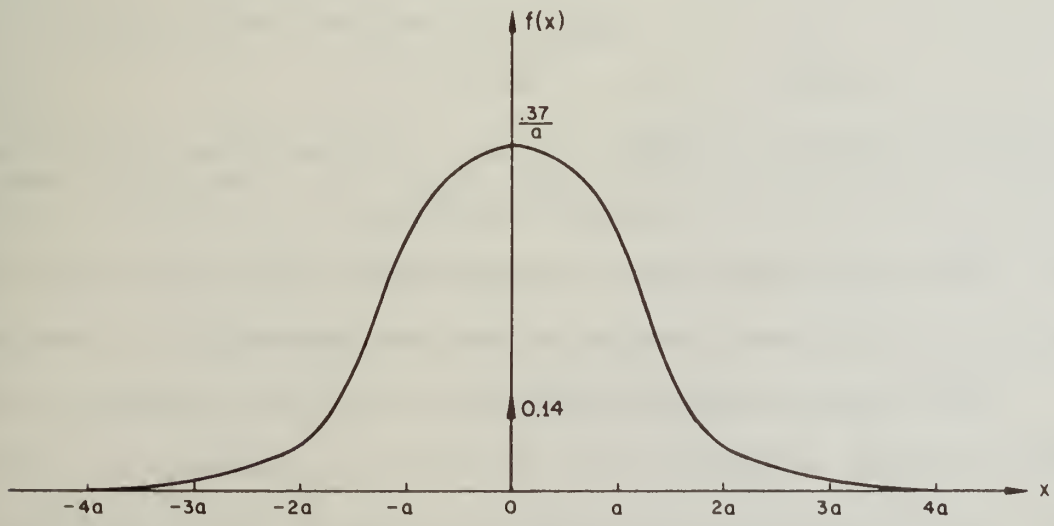

Figure 3.7 Density of $I_0(t)$ for $\rho T = 2.0$

$$\rho \frac{\partial w}{\partial t} = - \frac{\partial p}{\partial z} + \frac{\partial}{\partial x} \left(\mu \frac{\partial w}{\partial x} - \rho uw \right) + \frac{\partial}{\partial y} \left(\mu \frac{\partial w}{\partial y} - \rho vw \right) + \frac{\partial}{\partial z} \left(\mu \frac{\partial w}{\partial z} - \rho w^2 \right)$$

where ρ = density of the fluid

μ = viscosity of the fluid

p = pressure

In most references in fluid dynamics, turbulent flow is treated by considering the time averages of the parameters - velocity and pressure - so that the above equations are:

$$\frac{\partial \bar{u}}{\partial x} + \frac{\partial \bar{v}}{\partial y} + \frac{\partial \bar{w}}{\partial z} = 0$$

$$\rho \frac{\partial \bar{u}}{\partial t} = - \frac{\partial \bar{p}}{\partial x} + \frac{\partial}{\partial x} \left(\mu \frac{\partial \bar{u}}{\partial x} - \rho \bar{u}^2 - \rho \overline{u'^2} \right) + \frac{\partial}{\partial y} \left(\mu \frac{\partial \bar{u}}{\partial y} - \rho \bar{u}\bar{v} - \rho \overline{u'v'} \right) + \frac{\partial}{\partial} \left(\mu \frac{\partial \bar{u}}{\partial z} - \rho \bar{u}\bar{w} - \overline{u'w'} \right)$$

$$\rho \frac{\partial \bar{v}}{\partial t} = - \frac{\partial \bar{p}}{\partial y} + \frac{\partial}{\partial x} \left(\mu \frac{\partial \bar{v}}{\partial x} - \rho \bar{u}\bar{v} - \rho \overline{u'v'} \right) + \frac{\partial}{\partial y} \left(\mu \frac{\partial \bar{v}}{\partial y} - \rho \bar{v}^2 - \rho \overline{v'^2} \right) + \frac{\partial}{\partial z} \left(\mu \frac{\partial \bar{v}}{\partial z} - \rho \bar{v}\bar{w} - \rho \overline{v'w'} \right)$$

$$\rho \frac{\partial \bar{w}}{\partial t} = - \frac{\partial \bar{p}}{\partial z} + \frac{\partial}{\partial x} \left(\mu \frac{\partial \bar{w}}{\partial x} - \rho \bar{u}\bar{w} - \rho \overline{u'w'} \right) + \frac{\partial}{\partial y} \left(\mu \frac{\partial \bar{w}}{\partial y} - \rho \bar{v}\bar{w} - \rho \overline{v'w'} \right) + \frac{\partial}{\partial z} \left(\mu \frac{\partial \bar{w}}{\partial z} - \rho \bar{w}^2 - \rho \overline{w'^2} \right)$$

where $\bar{u}$, $\bar{w}$ and $\bar{v}$ indicate the averages

and u', w' and v' indicate the random portion

so that $u = \bar{u} + u'$ and so on.

It should be pointed out that the two sets of Navier-Stokes equations are identical, except for the additional components $\rho \overline{u'^2}$, $\rho \overline{v'^2}$, $\rho \overline{w'^2}$, $\rho \overline{u'v'}$, $\rho \overline{u'w'}$, $\rho \overline{v'w'}$ in the right side of the expressions. These factors are referred to as Reynold's stresses. Obviously, they are present only for turbulence.

In most cases, the solutions for the above set of equations are very difficult to find, particularly when the Reynold's stresses are included. These stresses are not well known either experimentally or theoretically. Graphs may be found for specific cases; however, they are dependent upon

many variables such as position, viscosity, shape of channel or pipe, and roughness of the walls of the channel or pipe.

In general, the Navier-Stokes equations may be written as

$$\frac{\partial u}{\partial t} + f(u, v, w) = a(x, y, z, t)$$

$$\frac{\partial v}{\partial t} + g(u, v, w) = b(x, y, z, t)$$

$$\frac{\partial w}{\partial t} + h(u, v, w) = c(x, y, z, t)$$

where f, g, h, a, b, c are functions of the corresponding variables. A simple case of these equations is called Langerin's equation which describes the motion of a free particle.

$$\frac{dv(t)}{dt} + \beta\, v(t) = n(t)$$

where n(t) is the driving function of the differential equation. In solutions for mean and autocorrelation function of v(t), n(t) is considered to be white noise with zero mean. Hence,

$$S_n(w) = \alpha$$

$$S_v(w) = \frac{\alpha}{w^2 + 2}$$

$$R_v(\tau) = \frac{\alpha}{2} e^{-\beta|\tau|}$$

and

$$f_v(v) = \sqrt{\frac{\beta}{4\pi\alpha}}\, e^{-\frac{\beta v^2}{4\alpha}}$$

The point here is that given information about the driving function, n(t), solutions of the mean and autocorrelation function of v(t) may be found. This statement is also true for the Navier-Stokes equations where a(s, y, z, t), b(x, y, z, t) and c(x, y, z, t) are the driving functions. The problem is that the equations are non-linear and thus, a closed-form solution is difficult to find.

4. IMPLEMENTATION OF THE TRANSDUCERS

4.1 Temperature Transducer

The obvious way to measure temperature is to construct a transducer which uses thermal noise. A transducer was built using a resistor as the (thermal) noise source. Figure 3.1 shows the block diagram. The basic problem with this transducer was that the amplitude of the noise source, the resistor, was too small and thus the amplifier was needed. However, the amplifier added undesirable noise and the resulting noise (the sum of the noise source and the amplifier noise) had an insufficient dependence upon the temperature.

Another transducer has more dependence on the temperature. This one uses a reversed-biased junction as the noise source. Shot noise is present but it is multiplied in the breakdown region by a factor of M where

$$M = \frac{1}{1 - (\frac{V}{V_B})^n}$$

and n = constant $(2 \leq n \leq 10)$

V = voltage across the junction

V_B = breakdown voltage

Thus, the noise has been amplified with no additional circuitry. Figure 4.1 shows the circuit configuration for this transducer. This transducer corresponds to a noise source, dependent upon the temperature, which has sufficient voltage to be input directly to a comparator. This voltage is compared with a DC voltage, V_A, and the output of the comparator is the stochastic sequence.

The calculations that follow show how this noise varies with respect to temperature. The operating point, I_C and V_{BC}, of the junction is determined by the solution of two equations which are represented in Figure 4.2. The linear equation, $I_C = \frac{V_{CC} - V_{BC}}{R}$, does not vary with respect to temperature. However, the remaining equation does and two variables, I_{CO} and V_B both depend upon temperature. So, differentiating

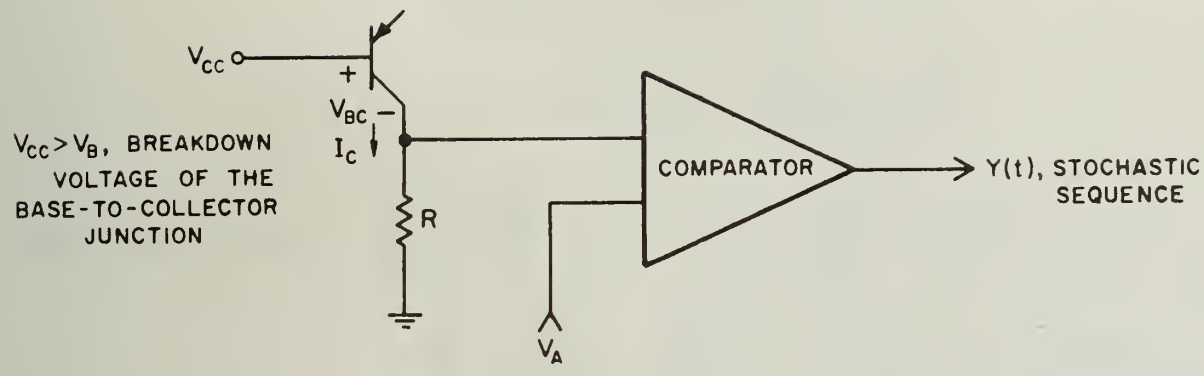

Figure 4.1 Circuit Diagram of the Temperature Transducer Using Shot Noise

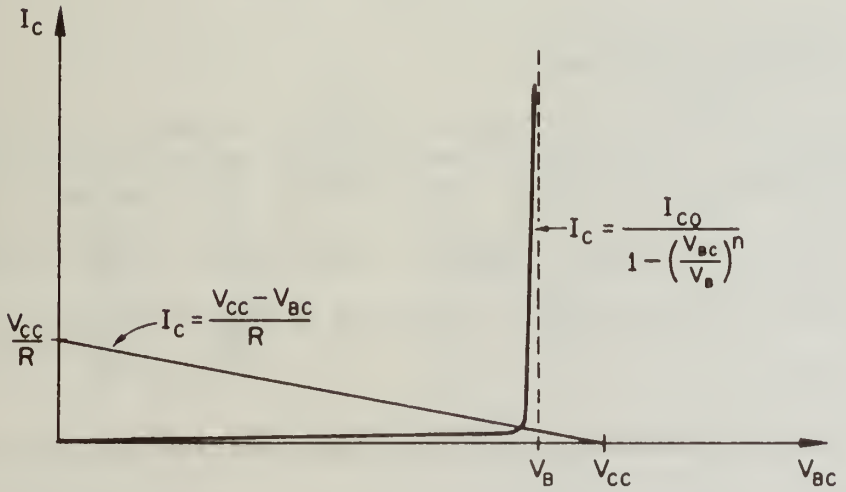

Figure 4.2 Graph of the Breakdown Region

$$\frac{dI_C}{dT} = \frac{dI_{CO}}{dT}\frac{1}{1-\delta^n} - \frac{nI_{CO}\,\delta^n}{V_B(1-\delta^n)^2}\frac{dV_B}{dT} \qquad \text{where } \delta = \frac{V_{BC}}{V_B}$$

$$= \frac{I_{CO}}{1-\delta^n}\left[\frac{1}{I_{CO}}\frac{dI_{CO}}{dT} - \frac{n\delta^n}{1-\delta^n}\frac{1}{V_B}\frac{dV_B}{dT}\right]$$

$$\simeq \frac{I_{CO}}{n\varepsilon}\left[\frac{1}{I_{CO}}\frac{dI_{CO}}{dT} - \frac{1}{\varepsilon V_B}\frac{dV_B}{dT}\right] \quad \text{for } \delta = 1-\varepsilon \text{ and } \varepsilon \ll 1.$$

It is known that $\frac{1}{I_{CO}}\frac{dI_{CO}}{dT}$ and $\frac{1}{V_B}\frac{dV_B}{dT}$ have the same order. Thus,

$$\frac{dI_C}{dT} \simeq -\frac{I_{CO}}{n\varepsilon^2 V_B}\frac{dV_B}{dT}$$

This implies the $\frac{dI_C}{dT}$ is negative and that the change in the breakdown voltage is much more significant than the change in the leakage current. The result is that the temperature and the noise power are inversely proportional (since the noise power is directly proportional to the leakage current). Thus, it is expected that the mean of stochastic sequence is inversely proportional to the temperature (if $V_A <$ mean of the noise).

4.2 Luminance Transducer

In this transducer a photo-transistor is used as a variable resistor at the input of an amplifier. The output noise of the amplifier is dependent upon the input impedance. Thus, the output noise of the amplifier varies with respect to the luminance. A design of this transducer is shown in Figure 4.3.

From the arrangement in Figure 4.3, calculations of input noise, E_{ni}, may be made. In the equivalent noise circuit, R is the resistance of the collector-to-emitter junction of the photo-transistor which is dependent upon the luminance. I_s is the shot noise resulting from the photo-diode and E_n

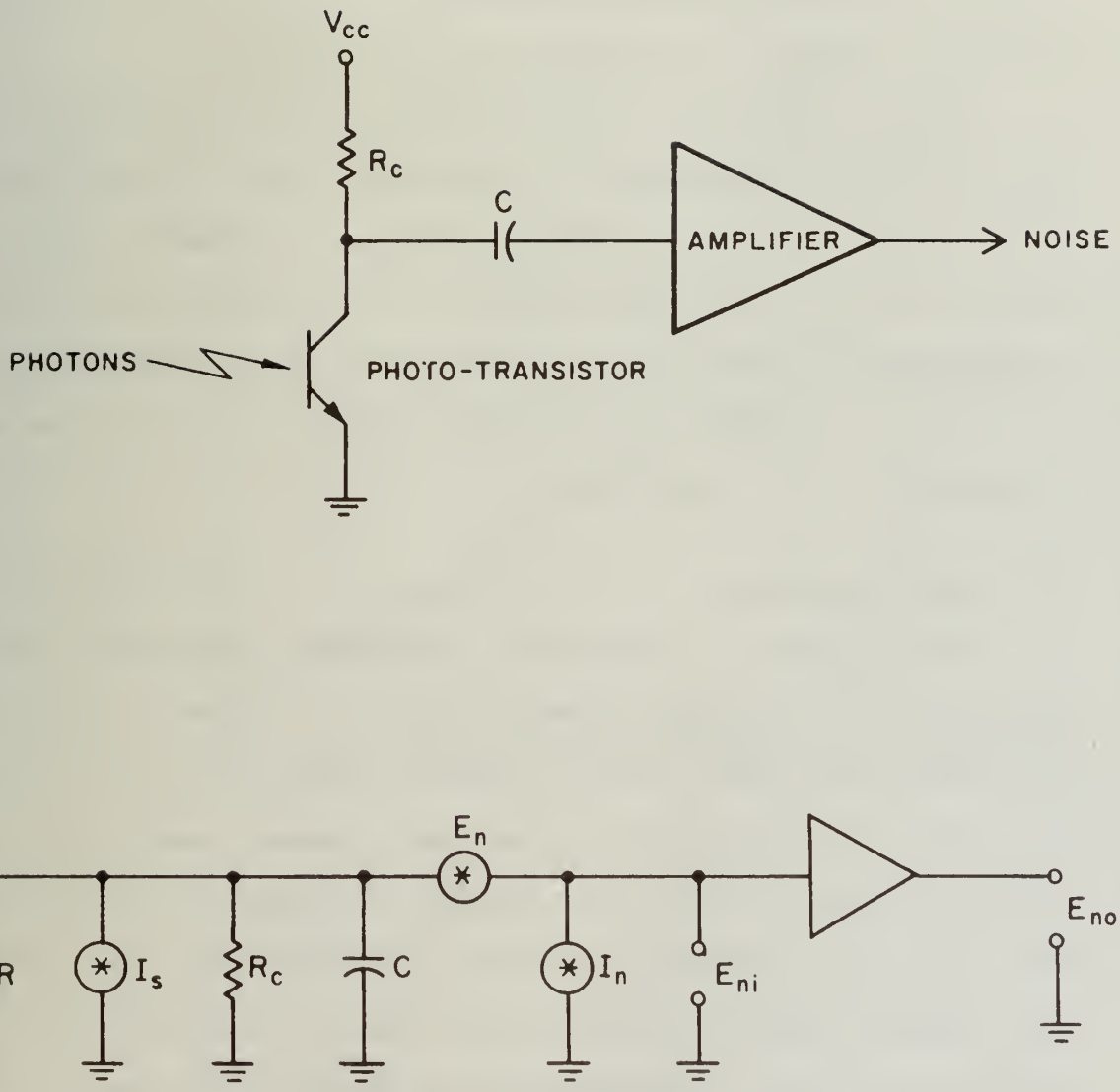

Figure 4.3 Configuration of the Noise Source for the Luminance Transducer and the Equivalent Noise Circuit

and I_n are the voltage and current noise, respectively, resulting from the amplifier. In most cases, I_n and E_n will be more significant than I_s.

$$E_{n_i}^2 = Z_p^2(I_s^2 + I_n^2) + E_n^2 \qquad \text{where } Z_p = R \| R_C \| (-jX_C)$$

The purpose of the capacitor is to block the DC voltage (low-pass filter); so that over the bandwidth of the amplifier, $X_C >> R_C$ and $X_C >> R$ and thus, $Z_p \simeq R \| R_C$. Figure 4.4 is a graph of E_{ni}^2 as R varies.

The one problem that is neglected in the above discussion is the range of the input resistance of the amplifier. After the input resistance becomes large enough, the feedback is sufficient to bring the amplifier into oscillation. Thus, a reasonable range for the input resistance is from 0 to R_C. Since the resistance, R, is the resistance of the photo-transistor and this resistance depends upon the luminance, the output noise of the amplifier is dependent upon the luminance.

4.3 Flow Transducer

This transducer is the easiest to implement. The reason is that the noise source is the natural phenomenon; that is, a transducer that measures the velocity of a laminar flow will output a random process in a turbulent flow. Thus, a method similiar to that used to measure laminar flow will be used here. Figure 4.5 shows the necessary ingredients for the flow transducer. The liquid enters at the left and strikes the obstacle. At this point, the flow becomes turbulent and the pressure transducer measures a random process which is dependent upon the average flow (volume rate of flow divided by the area of the tube). The item of interest is the fluctuating pressure measurement and not the average pressure. Thus, the pressure measurement (derived by the pressure transducer) is inserted into a comparator via a capacitor (low-pass filter). The resulting stochastic sequence then

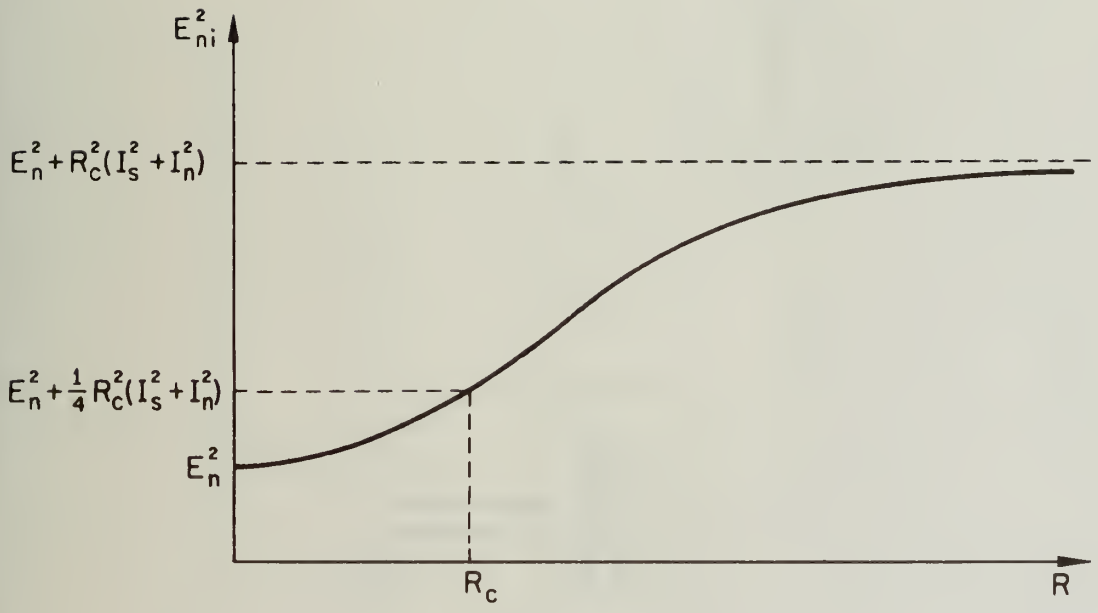

Figure 4.4 Graph of E_{ni}^2 vs. R

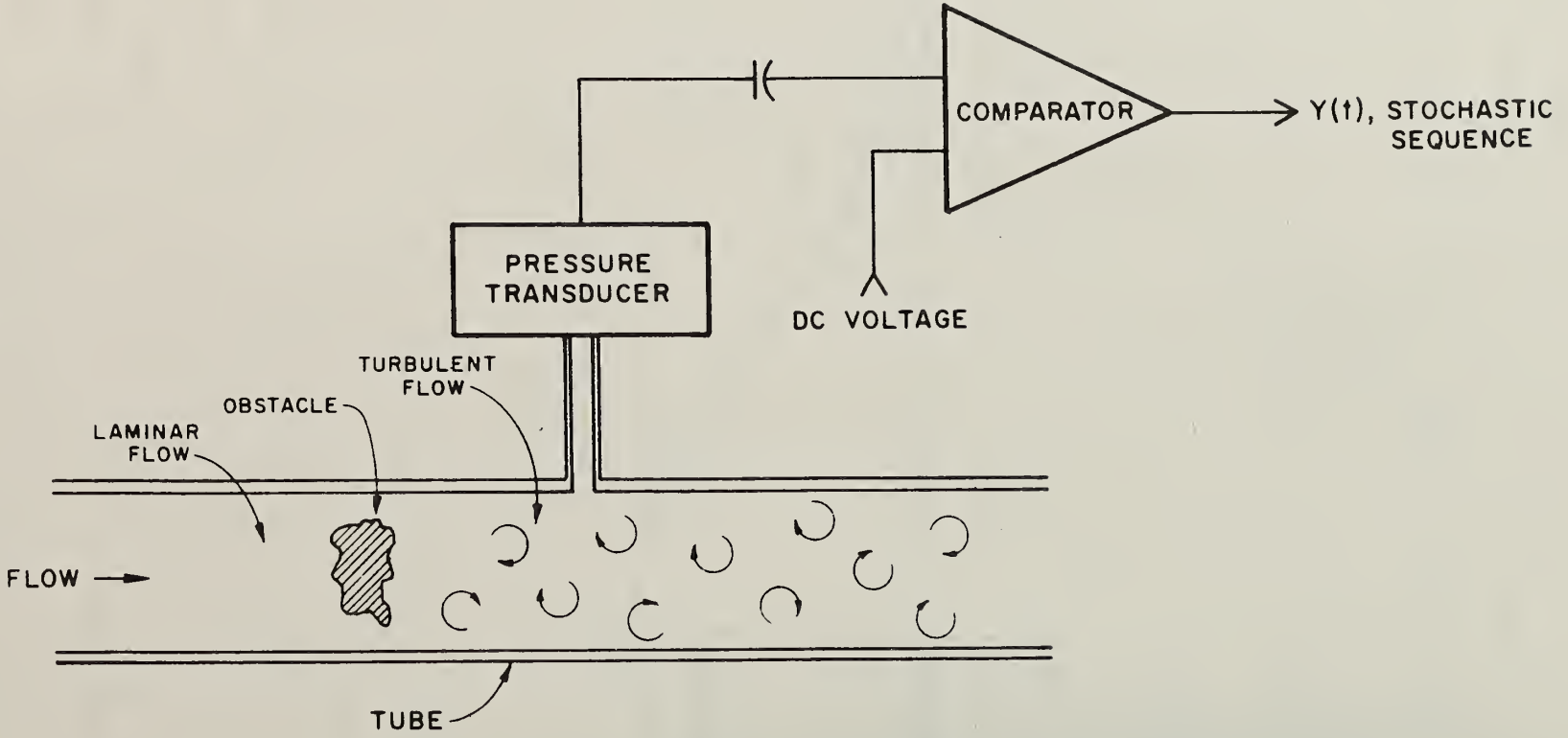

Figure 4.5 Arrangement for Flow Transducer

depends upon the velocity of the flow. Incidentally, the obstacle may be accomplished by a variety of methods: for example, by constricting the tube or possibly by bending the tube.

5. DATA AND RESULTS

5.1 Method of Measurement and Calculation of Errors

The determination of the time average of the stochastic sequence Y(t) via sampling was shown in Section 2.3. The algorithm used to obtain the time average is as follows:

1) sample Y(t) every λ seconds to obtain Y_k.

2) count the number of 1's, n, of Y_k in N time periods.

3) the time average of Y(t) is approximated by n/N.

First, it is necessary to assume that Y(t) is produced by a Markov process, which implies that Y_k is a Markov chain: a Markov process is a continuous process and a Markov chain is a discrete process. This assumption is not unreasonable since it may be shown that shot noise (Poisson process) and thermal noise (Wiener-Lévy process) are of the Markov type. Since Y(t) is a Markov process, the transition probability matrix, P(t), is

$$P(t) = \begin{bmatrix} \frac{b}{a+b} + \frac{a}{a+b} e^{-(a+b)t} & \frac{a}{a+b} - \frac{a}{a+b} e^{-(a+b)t} \\ \frac{b}{a+b} - \frac{b}{a+b} e^{-(a+b)t} & \frac{a}{a+b} + \frac{b}{a+b} e^{-(a+b)t} \end{bmatrix}$$

where $a\Delta + \mathcal{O}(\Delta)$ is the probability that Y(t) changes from 0 to 1 in the interval of time $(t, t+\Delta)$, $b\Delta + \mathcal{O}(\Delta)$ is the probability that Y(t) changes from 1 to 0 in the interval of time $(t, t+\Delta)$, and $\mathcal{O}(\Delta)$ is such that $\frac{\mathcal{O}(\Delta)}{\Delta}$ approaches zero as Δ approaches zero. It is known that the length of time, T_i, that is spent in state i is exponentially distributed.

$$f_{T_0}(t) = a\, e^{-at} \qquad \text{for} \quad t \geq 0$$

and

$$f_{T_1}(t) = b\, e^{-bt} \qquad \text{for} \quad t \geq 0$$

Now, if Y(t) is sampled every λ seconds, the corresponding sequence Y_k is a Markov chain with a probability transition matrix

$$P = \begin{bmatrix} 1 - \Delta_1 & \Delta_1 \\ \Delta_2 & 1 - \Delta_2 \end{bmatrix}$$

where $\Delta_1 = 1 - e^{-a\lambda}$ and $\Delta_2 = 1 - e^{-b\lambda}$.

The number of time periods, N_i, that are spent in state i is geometrically distributed:

$$P(N_0 = n) = \Delta_1(1 - \Delta_1)^n \qquad \text{for} \quad n = 0, 1, \ldots$$

and $$P(N_1 = n) = \Delta_2(1 - \Delta_2)^n \qquad \text{for} \quad n = 0, 1, \ldots$$

Using the above equations, it is easy to determine the error of the approximation, $Y(t) \sim Y_k$. The pulse-widths of $Y(t)$ and Y_k will now be compared. (The pulse width is the time that $Y(t)$ or Y_k is equal to 1). The expected pulse width, T_1, of $Y(t)$ is

$$E\{T_1\} = \int_0^\infty b\, t\, e^{-bt}\, dt$$

$$= \frac{1}{b}$$

The expected pulse width, λN_1, of Y_k is

$$\lambda E\{N_1\} = \lambda \sum_{n=0}^{\infty} n\, \Delta_2(1 - \Delta_2)^n$$

$$= \lambda \frac{1 - \Delta_2}{\Delta_2}$$

$$= \lambda \frac{e^{-b\lambda}}{1 - e^{-b\lambda}}$$

If λ is chosen so that $e^{-b\lambda} \simeq 1 - b\lambda$ ($\Rightarrow 0 < b\lambda \ll 1$), then

$$\lambda E\{N_1\} \simeq \frac{1 - b\lambda}{b} \simeq \frac{1}{b}$$

Note that the expected pulse widths of $Y(t)$ and Y_k are approximately the

same if λ is chosen properly; i.e., $b\lambda << 1$. The mean square error, $E\{(T_1 - \lambda N_1)^2\}$, is more interesting:

$$E\{(T_1 - \lambda N_1)^2\} = E\{T_1^2\} + \lambda^2 E\{N_1^2\} - 2\lambda E\{T_1 N_1\}$$

$$= \frac{2}{b^2} + \lambda^2 \frac{(1 - \Delta_2)(2 - \Delta_2)}{\Delta_2^2} - 2\lambda \frac{(1 - \Delta_2)(\lambda + \frac{\Delta_2}{b})}{\Delta_2^2}$$

$$= \frac{2}{b^2} - \frac{\lambda(1 - \Delta_2)(\lambda + \frac{2}{b})}{\Delta_2}$$

Again, assuming that λ is chosen such that $e^{-b\lambda} \simeq 1 - b\lambda$,

$$E\{(T_1 - \lambda N_1)^2\} \simeq \frac{2}{b^2} - \frac{\lambda(1 - b\lambda)(\lambda + \frac{2}{b})}{b\lambda}$$

$$= \frac{\lambda}{b} + \lambda^2 \simeq \frac{\lambda}{b}$$

Thus, the smaller the sampling period, the closer Y_k fits $Y(t)$. (Intuitively, this result is expected). By using Tchebycheff's inequality,

$$P\{|T_1 - \lambda N_1| > \eta\} \leq \frac{\lambda}{b\eta^2}$$

It is possible to use this equation as a measure of the error in the approximation $Y(t) \sim Y_k$.

A more important consideration is the error in using the time average of the sampled data Y_k. This error was discussed in section 3.3. It was concluded that $\frac{1}{T}\int_0^T Y(t)dt$ is "optimally approximated" by $\sum_{k=1}^{N} a_k Y_k$ where $T = N\lambda$ if the equations $\frac{1}{N\lambda}\int_0^{N\lambda} R(t - n\lambda)dt = \sum_{k=1}^{N} a_k R[(k - n)\lambda]$ for $n = 1, 2, \ldots, N$ are satisfied. (The term "optimally approximated" means minimum mean square error...)

As described in the algorithm above, each sample Y_k is given equal weight ($\Rightarrow a_k = \frac{1}{N}$ for $k = 1, 2, \ldots, N$). The reason for this assignment of

a_k is mainly to simplify the design of the stochastic meter described in section 5.2. However, as explained in section 3.3, by carefully choosing the sampling rate, λ, the mean square error of the time averages may be made as close to the minimum mean square error as necessary. Mathematically, the mean square error, e, is

$$e = E\{(\frac{1}{N\lambda}\int_0^{N\lambda} Y(t)dt - \frac{1}{N}\sum_{k=1}^{N} Y_k)^2\}$$

$$= \frac{1}{N\lambda}\int_0^{N\lambda}(1 - \frac{t}{N\lambda})\,R(t)dt + \frac{1}{N}R(0) + \frac{2}{N}\sum_{k=1}^{N-1}(1 - \frac{k}{N})\,R(k\lambda) - \frac{2}{N^2\lambda}\sum_{k=1}^{N}\int_0^{N\lambda} R(t - k\lambda)dt$$

Consider that λ is chosen so that for some $\varepsilon > 0$, the equation

$$\left|\int_0^{N\lambda} R(t)dt - \lambda\sum_{k=0}^{N-1} R(k\lambda)\right| \leq \varepsilon$$

or, equivalently,

$$\left|\frac{1}{N\lambda}\int_0^{N\lambda} R(t)dt - \frac{1}{N}\sum_{k=0}^{N-1} R(k\lambda)\right| \leq \frac{\varepsilon}{N\lambda}$$

is satisfied. Referring to section 3.3, this condition implies that

$$|R(t + \lambda) - R(t)| \leq \frac{\varepsilon}{N\lambda}$$

It is obvious that the equations used for solving the a_k's are nearly satisfied. Intuitively, it is expected that the minimum mean square error, e_m, (as defined in section 2.3) would be approached as $\varepsilon \to 0$. Calculations confirm this notion.

$$e = e_m - E\{(\frac{1}{T}\int_0^{T} Y(t)dt - \frac{1}{N}\sum_{k=1}^{N} Y_k)\,\frac{1}{N}\sum_{k=1}^{N} Y_k\}$$

$$= e_m + \frac{1}{N^2}\sum_{k=1}^{N}\sum_{n=1}^{N} R((k-n)\lambda) - \frac{1}{NT}\sum_{k=1}^{N}\int_0^{T} R(t - k\lambda)dt$$

$$= e_m + \frac{1}{N} \sum_{k=1}^{N} \left[\frac{1}{N} \sum_{n=1}^{N} R((k-n)\lambda) - \frac{1}{T} \int_0^T R(t - k\lambda)dt\right]$$

$$\leq e_m + \frac{\varepsilon}{N\lambda}$$

Remember that ε was chosen arbitrarily and that λ resulted from ε. Also, note that the error, e, can be made very small by increasing N to be a large number.

There is one remaining calculation. It is known that $\lim_{N\to\infty} \hat{A}_N(Y) = \mu_Y$, since Y_k is ergodic. But if the sampling is finite, the mean-square error becomes

$$E\{(\hat{A}_N(Y) - \mu_Y)^2\} = \frac{1}{N} R(0) + \frac{2}{N^2} \sum_{k=1}^{N-1} (N - k)\, R(k\lambda) - \mu_Y^2$$

$$= \frac{1}{N} [R(0) - \mu_Y^2] + \frac{2}{N} \sum_{k=1}^{N-1} (1 - \frac{k}{N})[R(k\lambda) - \mu_Y^2]$$

$$= \frac{1}{N} C(0) + \frac{2}{N} \sum_{k=1}^{N-1} (1 - \frac{k}{N})\, C(k\lambda)$$

$$\text{where} \quad C(k\lambda) = R(k\lambda) - \mu_Y^2$$

Obviously, as N becomes larger, the mean square error becomes smaller. Neglecting the second term on the right side of the equation above and maximizing, Tchebycheff's inequality becomes

$$P\{|\hat{A}_N(Y) - \mu_Y| > \eta\} < \frac{1}{2N\eta^2}$$

This expression gives a measure of the accuracy of the resulting time average, $\hat{A}_N(Y)$.

5.2 Implementation of the Stochastic Meter

In the previous section, an algorithm was given to obtain the time average of Y(t). From this algorithm and several design specifications, a

meter, called a stochastic meter, that can determine the time average of a random process can be constructed. Figure 5.1 shows a block diagram of the stochastic meter. Since this meter must accept a variety of inputs from the various transducers, a buffer which is a high impedance, wide bandwidth, low gain amplifier is the first stage. A variable gain amplifier and a variable DC level control for the comparator is available for experimental purposes. The comparator converts the input into a stochastic sequence. Note that the comparator is actually part of the transducer in the previous discussions. However, in order to have versatility, these circuits are included in the stochastic meter.

The algorithm for obtaining the time average is implemented by the remaining circuitry which is digital (TTL). The 10 MHz master clock is used to sample the resulting stochastic sequence from the comparator and, also, to determine the length of the averaging period (λN). In order to avoid dividing the contents of the two counters (one with n and the other with N), the averaging period counter has a multiple of ten. Then the number, n, may be displayed directly and the decimal point is placed according to the averaging period.

A justification of the 10 MHz master clock is needed. As shown in previous calculations the smaller the sampling period, the "better" the approximation of the sampled time average. In section 5.1, it was indicated that if the sampling period, λ, was chosen so that

$$|R(t + \lambda) - R(t)| \leq \frac{\varepsilon}{N\lambda} \qquad \text{for all } t$$

then the mean square error, e, is

$$e \leq e_m + \frac{\varepsilon}{N\lambda}$$

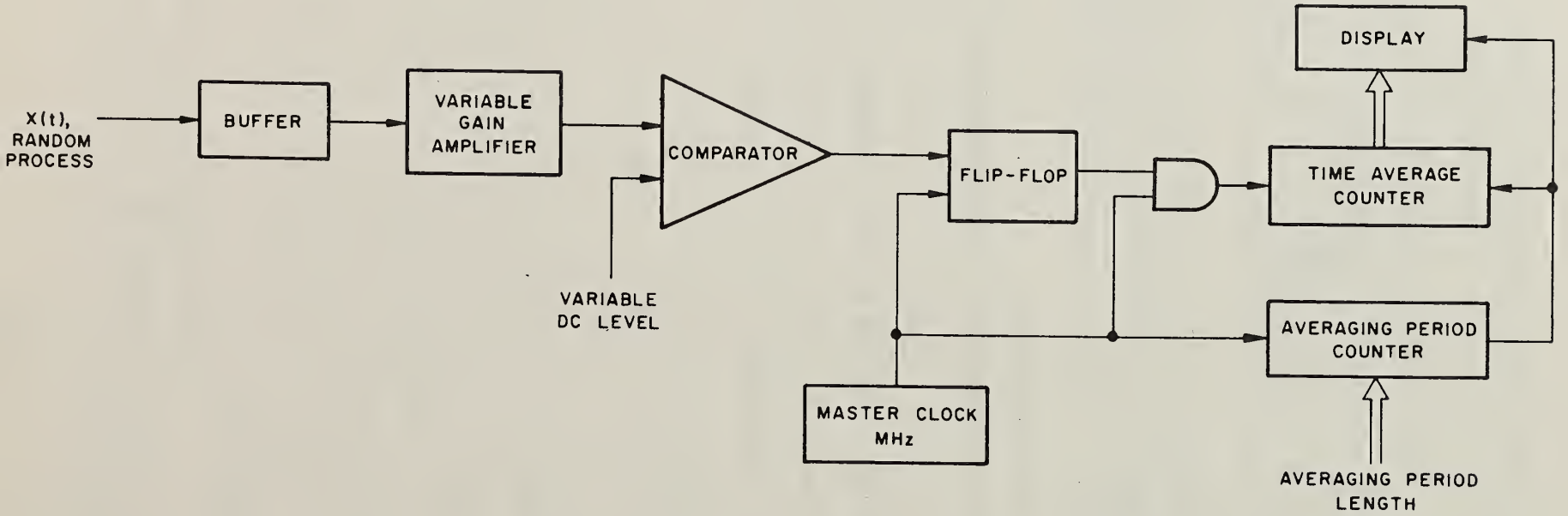

Figure 5.1 Block Diagram of the Stochastic Meter

where e_m = minimum mean square error. In section 3.1, calculations were made assuming that the noise source was thermal noise (flat power spectrum and Gaussian distributed). The calculations for $R_Y(\tau)$ are very complicated and it was not presented in a closed form (rather $R_Y(\tau)$ was expressed as an integral). However, an approximation may be made:

$$R(\tau) = \int_A^\infty \int_A^\infty f(x_1, x_2; \tau)\, dx_1\, dx_2$$ where $f(x_1, x_2; \tau)$ = Gaussian density with correlation coefficient, $r(\tau) = e^{-\alpha|\tau|}$

But, $$R(0) = \int_A^\infty \int_{-\infty}^\infty f(x_1, x_2; \tau)\, dx_1\, dx_2$$

Therefore, $$R(0) - R(\lambda) = \int_A^\infty \int_{-\infty}^A f(x_1, x_2; \tau)\, dx_1\, dx_2$$

This integral may be approximated when $r(\lambda) \simeq 1$ (which is the case when $\lambda << 1$).

$$|R(0) - R(\lambda)| \simeq e^{-\frac{A^2}{2\sigma^2}} \frac{\cos^{-1} r(\lambda)}{2\pi}$$

This implies that $$e^{-\frac{A^2}{2\sigma^2}} \frac{\cos^{-1} r(\lambda)}{2\pi} \leq \frac{\varepsilon}{N\lambda}$$

The constants now need to be given values. The constant, A, is the DC level of the comparator. The comparator takes values from $0.1\sigma < A < 4\sigma$, but in most cases $A \simeq \sigma$. The constant, $N\lambda$, is the averaging period, and it varies from $10^{-3} \leq N\lambda \leq 10$, with the most common value being $N = 1$. The constant, $\frac{\alpha}{2\pi}$, is the corner frequency of the amplifiers in front of the comparator and $\alpha = 5 \times 10^5$. The constant, ε, is an error parameter and may be chosen so that the last equation in section 2.3 is satisfied. A table is given for various sampling.

λ	$f = \frac{\cos^{-1} r(\lambda)}{2\pi}$	$fe^{-.005}$	fe^{-1}
10^{-7}	0.05	0.05	.018
10^{-8}	0.016	0.016	.006

These data imply that if $\lambda = 10^{-7}$, ε must be greater than 0.05. This value for ε is satisfactory, so the 10 MHz clock was chosen. Obviously, there is a trade-off involved. The practical considerations are that the comparator output has a non-zero rise-time and fall-time and the input noise frequency spectrum is not necessarily flat so that the corner frequency may be lower. It is not necessary to have a sampling rate much greater than the rise-time of the comparator output.

Appendix I shows the characteristics of the stochastic meter.

5.3 Data and Results

This section shows the data that was obtained from the transducers described in section 4 and shown in detail in Appendix B. The data and experimental procedures that are used to obtain the graphs in this section are presented in Appendix C.

The graphs in Figures 5.2 and 5.3 show the data from two temperature transducers: one using thermal noise and the other using a reverse-biased junction. The thermal noise temperature transducer does not respond according to the theory presented in section 3.1. In particular, the graph, Figure 5.2, does not resemble Figure 3.2; i.e., the time average increases as temperature increases in Figure 3.2 while the time average decreases as temperature increases in Figure 5.2. The cause of this discrepancy is that the response of the amplifier as the temperature changes was not considered in the theory. Obviously, the gain of the amplifier decreases as the

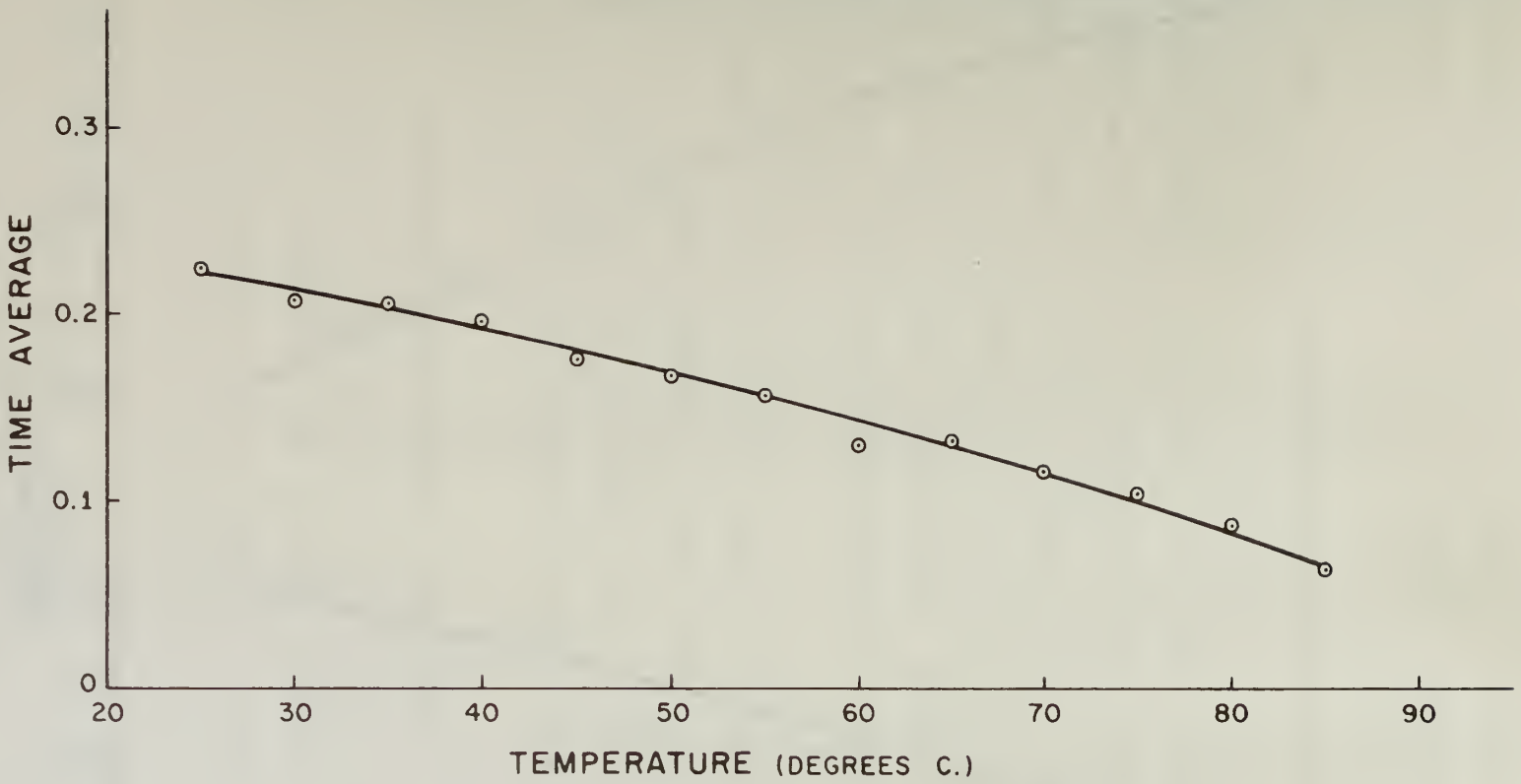

Figure 5.2 Graph of the Thermal Noise Temperature Transducer

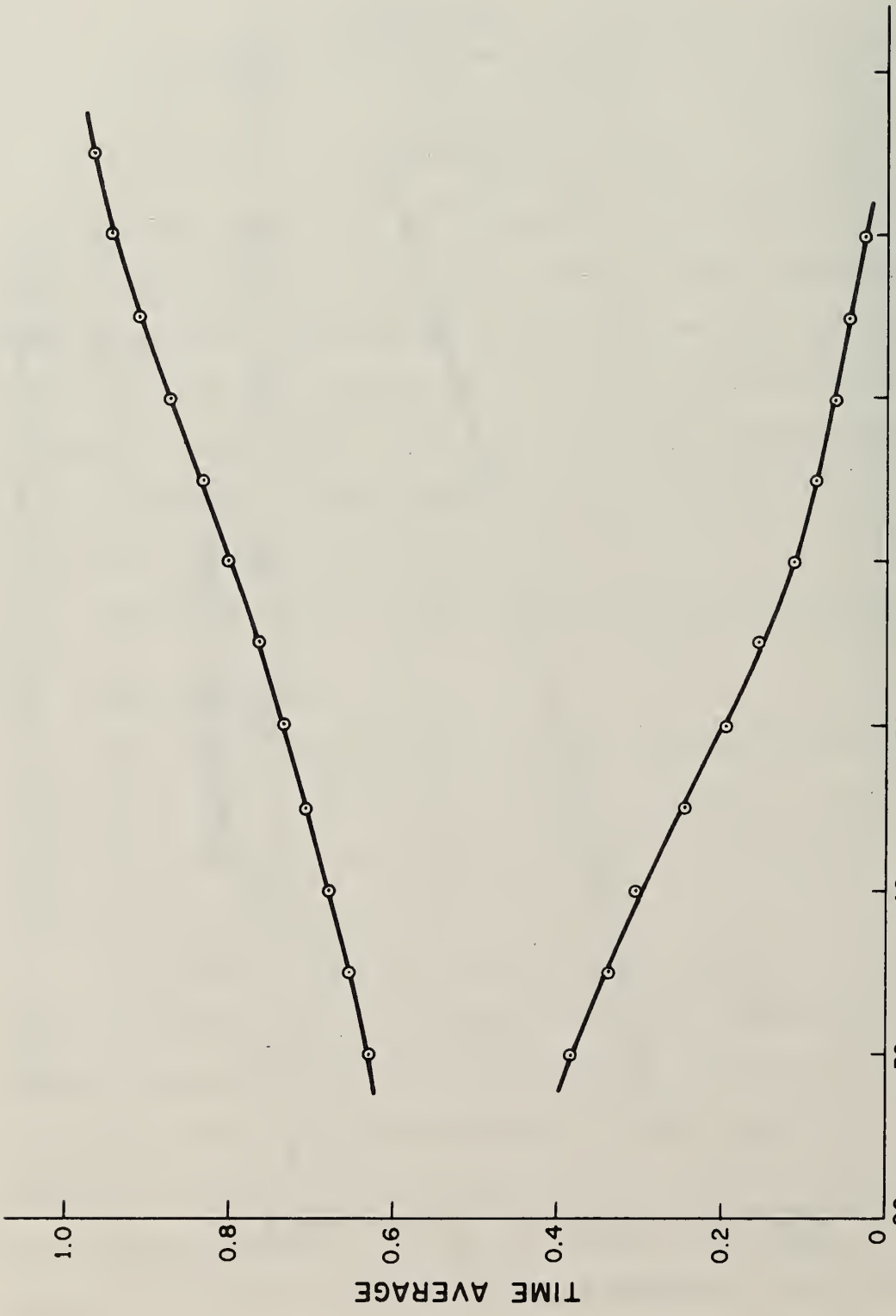

Figure 5.3 Graph of the Shot Noise Temperature Transducer

temperature increases and it is sufficient to offset the increase in amplitude of the thermal noise. Note that the slope of the graph is rather small.

In Figure 5.3 the graph of the temperature transducer using the reverse-bias junction is shown. This graph shows the expected results as discussed in section 4.1. An interesting characteristic of this graph is that there are two curves shown--one above and one below the time average of one half--and these curves are asymmetrical. The reason is that the density of this random process (the shot noise resulting for the reverse-bias junction) is not symmetrical around its mean. Therefore, two different curves result. Setting the DC level of the comparator below the mean gives the result shown in the lower curve and vice-versa. Incidentally: Changing the value of the resistor from the collector to V_{CC}^{-} varies the slope of the curves (they are inversely proportional).

The graphs in Figures 5.4 and 5.5 show the results of the luminance transducer. Two procedures were used to obtain these graphs.

1) An incandescent light bulb whose line voltage is varied and a narrow band light filter are used in conjunction to obtain Figure 5.3.

2) An incandescent light bulb whose line voltage is fixed and whose distance to the transducer is varied is used to obtain Figure 5.4.

Note that the incandescent light bulb has the property that the spectral radiant energy distribution does not maintain a constant shape as the voltage is varied, thus, a narrow band wavelength filter is used to minimize this problem. In the case of a fixed voltage and varying distance (of the transducer to the light bulb) it was necessary to maintain a consistent direction in both the transducer and the light bulb; i.e., in moving the transducer (or in moving the light bulb) the direction that it was pointing

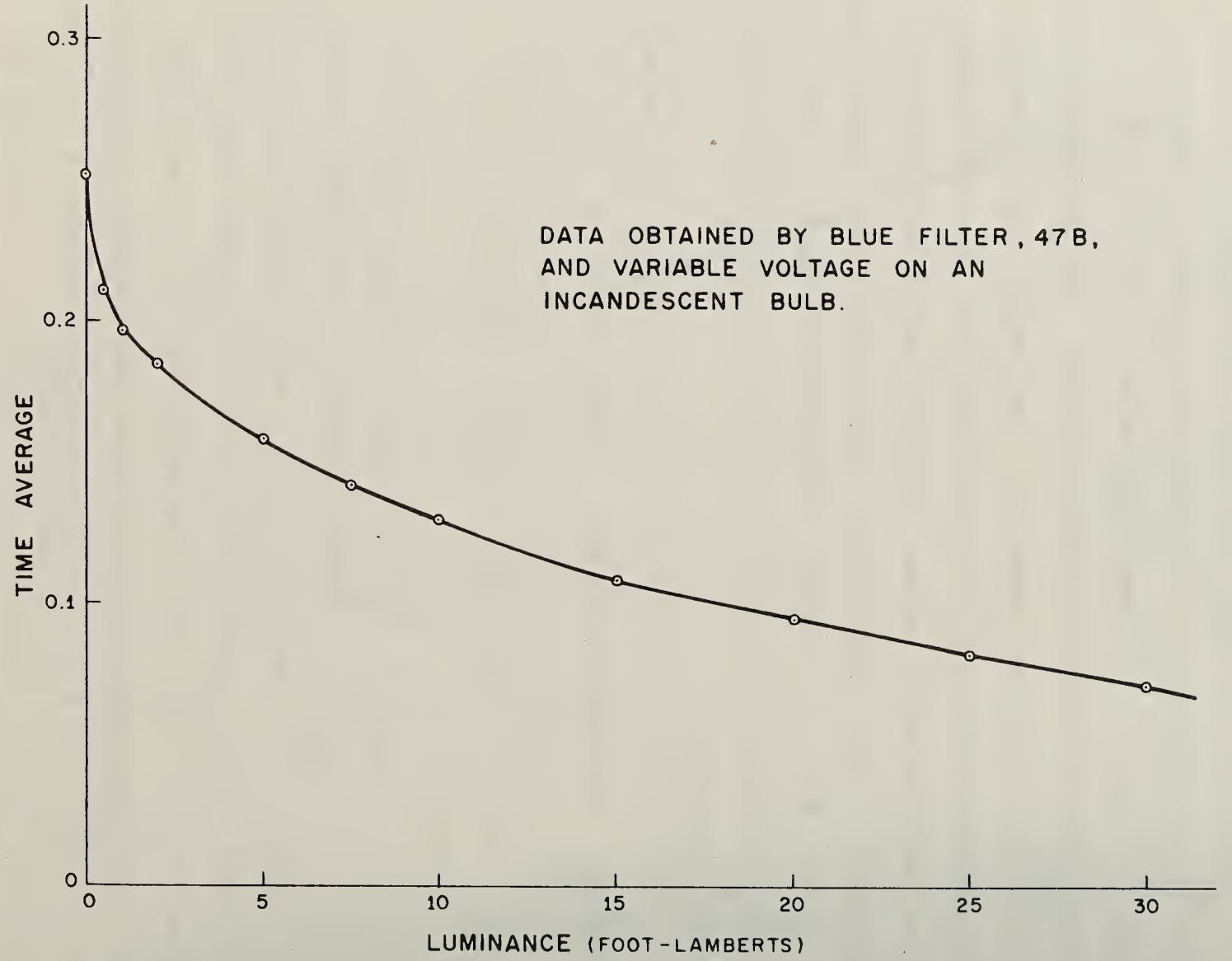

Figure 5.4 Graph of the Luminance Transducer, Part A

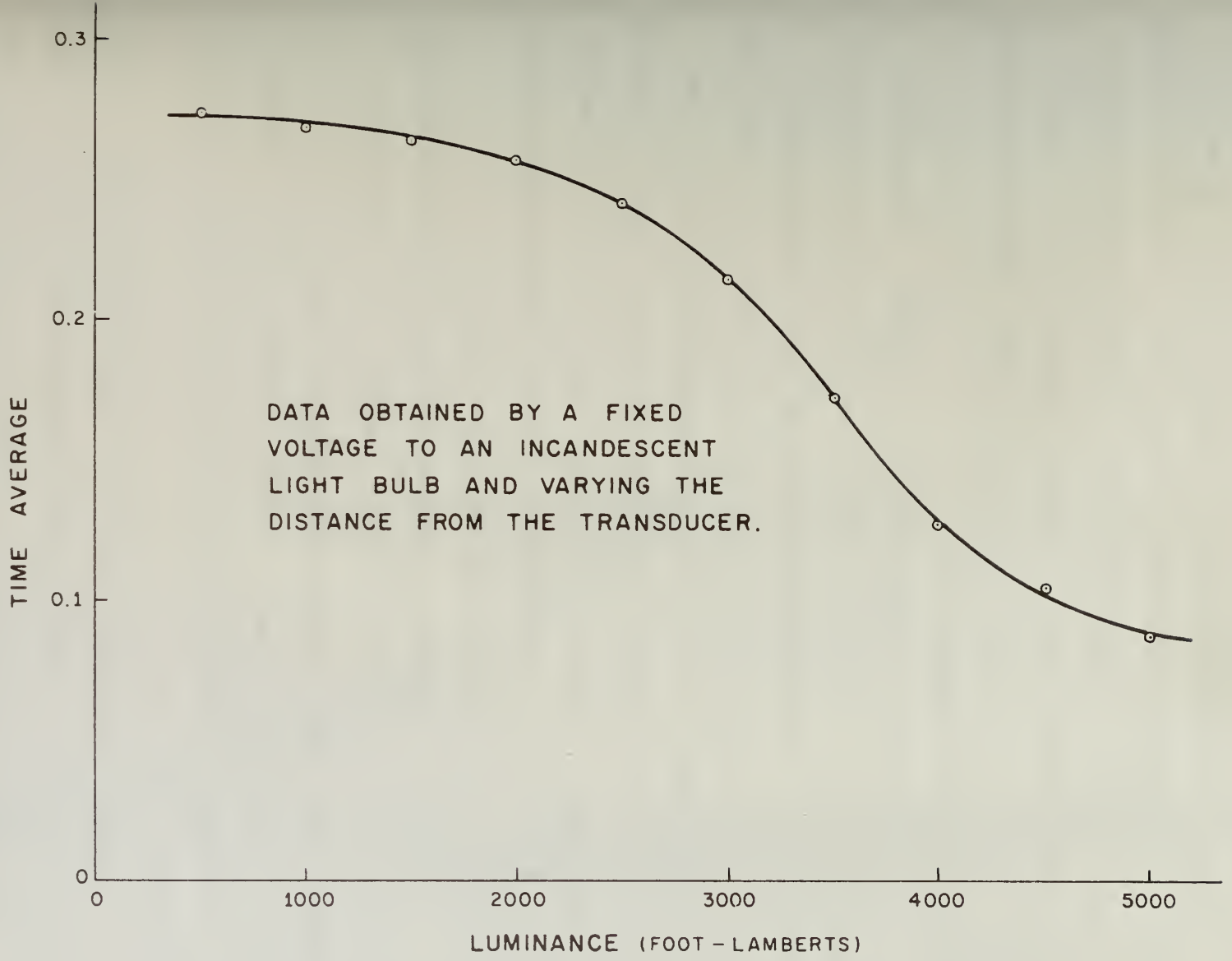

Figure 5.5 Graph of the Luminance Transducer, Part B

must be maintained, especially when the transducer is placed very close to the light bulb. This procedure is discussed in detail in Appendix C.

The goal of these procedures is to maintain a consistent spectral energy distribution while varying the luminance (i.e., to maintain the shape of the spectrum). Because the spectral distribution has two distinct shapes in each of these cases, the graphs in Figures 5.4 and 5.5 are different. In both cases, however, the resulting graphs are expected and agree with the discussion in section 4.2.

Figure 5.6 shows the graph of the flow transducer. The basic construction is shown in Figure 4.5. The tube was a 1/2 inch inside diameter plexiglass tube. The obstacle was constructed in the following manner: 1) the tube was divided into two parts by a perpendicular cut, 2) a 3/8 inch hole was placed in a 1/4 inch thick plexiglass sheet, and 3) the plexiglass sheet was epoxied to both parts of the tube so that the 3/8 inch hole was centered. The pressure transducer was placed downstream from the obstacle (about 1 inch). The remaining details of this transducer and the procedure in obtaining the data are explained in Appendix C.

As mentioned in Appendix C problems arose from obtaining additional data points for the graph in Figure 5.6. However, it is reasonable to assume that this graph is a good representation. Note that there is a similiarity in Figures 5.6 and 5.4 (if the horizontal axis is reversed). This similiarity is expected since both of the noise sources are Gaussian distributed.

One more comment about the flow transducer should be made. As noted in Appendix C, the time period of the stochastic meter is set at 10 seconds. (All other readings were made at a one second time period). A longer time period was necessary because low frequencies (< 100 Hz) dominated the power

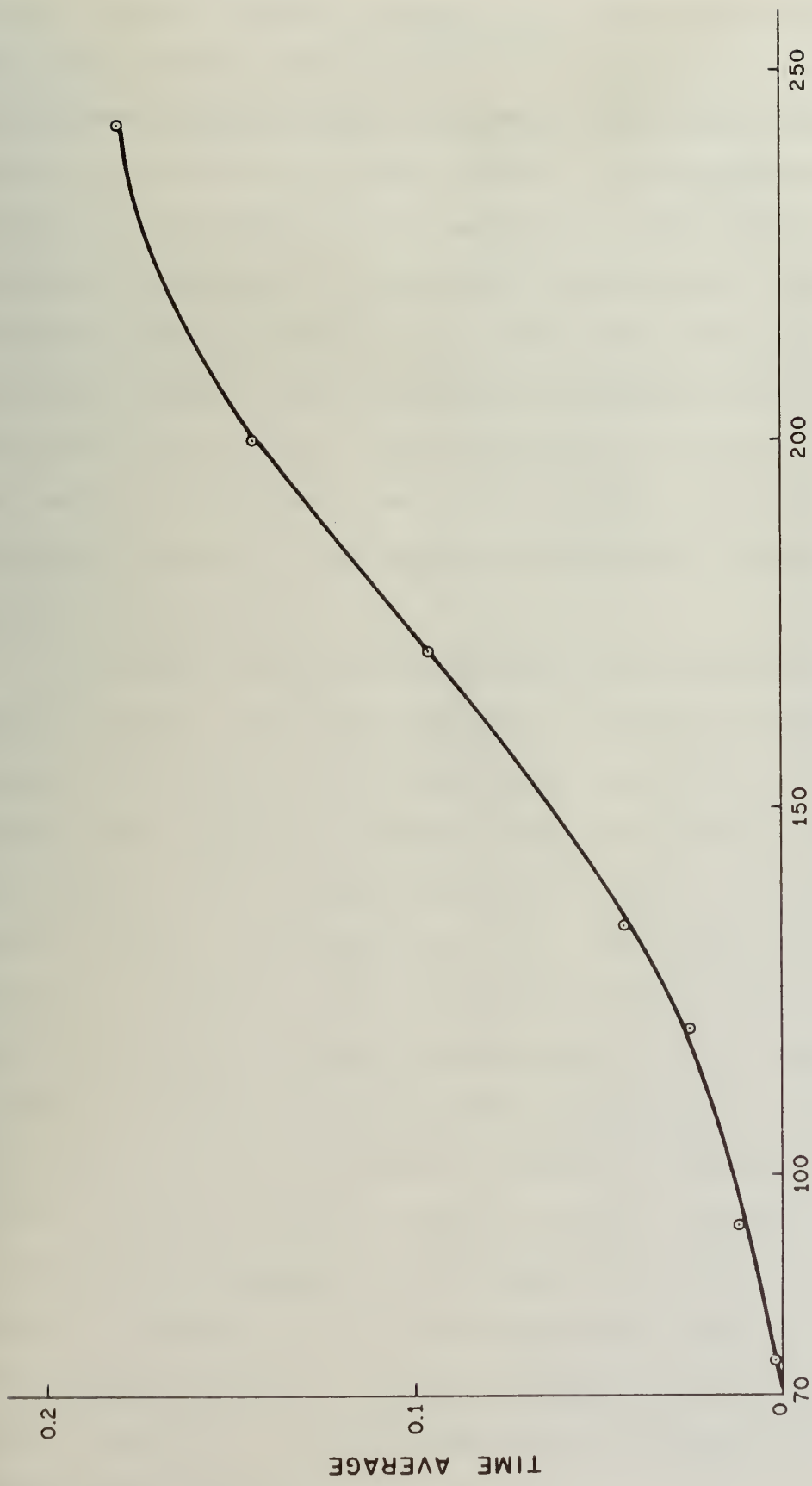

Figure 5.6 Graph of the Flow Transducer

spectrum of the noise source. The resulting stochastic sequence would have long lengths of time (in the order of milliseconds or more) in which the sequence was in state 0 or 1. Thus, the longer averaging period gives a better time average.

6. CONCLUSIONS

From the theory and the actual implementation of these transducers it can be concluded that the basic concept of Molecular Stochastics is feasible. Both theoretically and realistically, these transducers may be constructed and there is a relationship between the time average of the stochastic sequence and the physical variable that is being measured. In every case that was realized (temperature, luminance and flow transducers) this relationship was not a linear function but it was one-to-one, continuous, and may be considered linear in smaller ranges. In every case, the relationship between the time average and the physical parameter being measured was predicted.

A secondary concern of this project was the simplicity and cost of these transducers. One of the advantages of stochastic computing is the simplicity and economy of the arithmetic unit and so, the goal was to maintain these properties in the transducers. The transducers have, at most, an amplifier and a comparator along with a sensor (which may be a resistor, transistor, photo-transistor, etc.). The minimum amount of circuitry is a comparator. In the transducers described in this paper, the shot noise temperature transducer would require the least amount of circuitry: a reverse biased base-to-collector junction (the sensor), one stage amplifier (one transistor), and one comparator (available in integrated circuits). A digital temperature transducer normally would use a thermistor as a sensor and a A/D converter to convert the analog signal into a digital result. An A/D converter is much more complex and expensive than a comparator and an amplifier combined. The point is that the transducers with the stochastic output yield a simplicity in transducer design (the A/D converter is eliminated and replaced with a comparator).

Although this paper covers the implementation of three different transducers, it is felt other kinds of transducers may be built. One that already has been built is the Geiger Counter. Other possibilities are transducers that measure voltage and current. As mentioned in Appendix B, the amplitude of the shot noise resulting from the reverse-biased junction is dependent upon the voltage across the junction. The range of voltage dependence is small, however (about 5 volts). Obviously, if a successful voltage transducer were constructed, the current transducer would follow immediately.

APPENDIX A

Specifications of the Stochastic Meter

The circuit diagrams of the stochastic meter are given in Figures A-1 through A-5. In Figure A-6, the frequency response of the buffer and variable amplifier is given. This figure was used in section 5.2 to determine the constant α. The frequency response curve was obtained by using a sine wave input at different frequencies. The input and output amplitudes were measured and the gain (in dB) was then determined.

In Table A-1, the accuracy of the stochastic meter is shown. In one case, the DC level of the comparator is fixed (so that the time average is about 0.4) and the frequency of the input signal (the sine wave) is varied. In the other case, the frequency of the input signal is fixed (~ 10 KHz) and the DC level of the comparator is varied. The mean and standard deviation for each case were calculated from ten samples, S_i, by the formulas:

$$\text{Mean} = \frac{1}{10} \sum_{i=1}^{10} S_i$$

$$\text{Standard Deviation} = \sqrt{\frac{10}{9} \left[\frac{1}{10} \sum_{i=1}^{10} S_i^2 - (\text{mean})^2\right]}$$

Note that the meter has an accuracy of 3^+ digits and when the slope of the input signal as it passes that threshold level is maximum, the accuracy is the best.

Figure A-7 shows the front view of the stochastic meter.

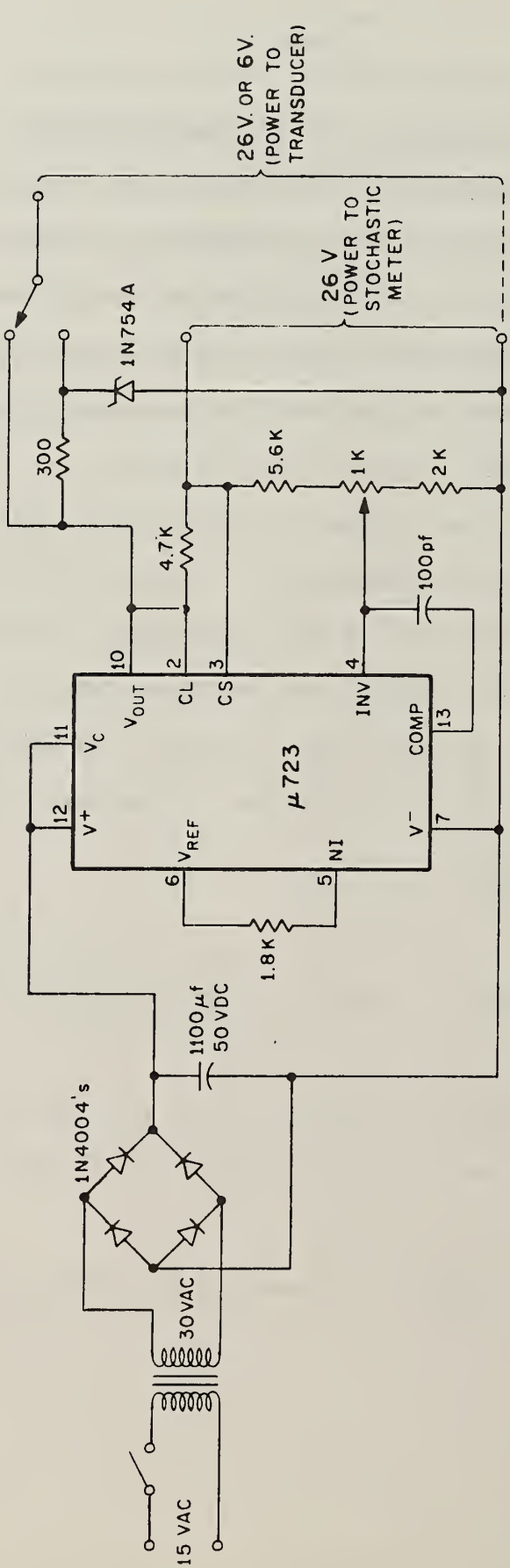

Figure A-1. Circuit Diagram of the Power Supply of the Stochastic Meter

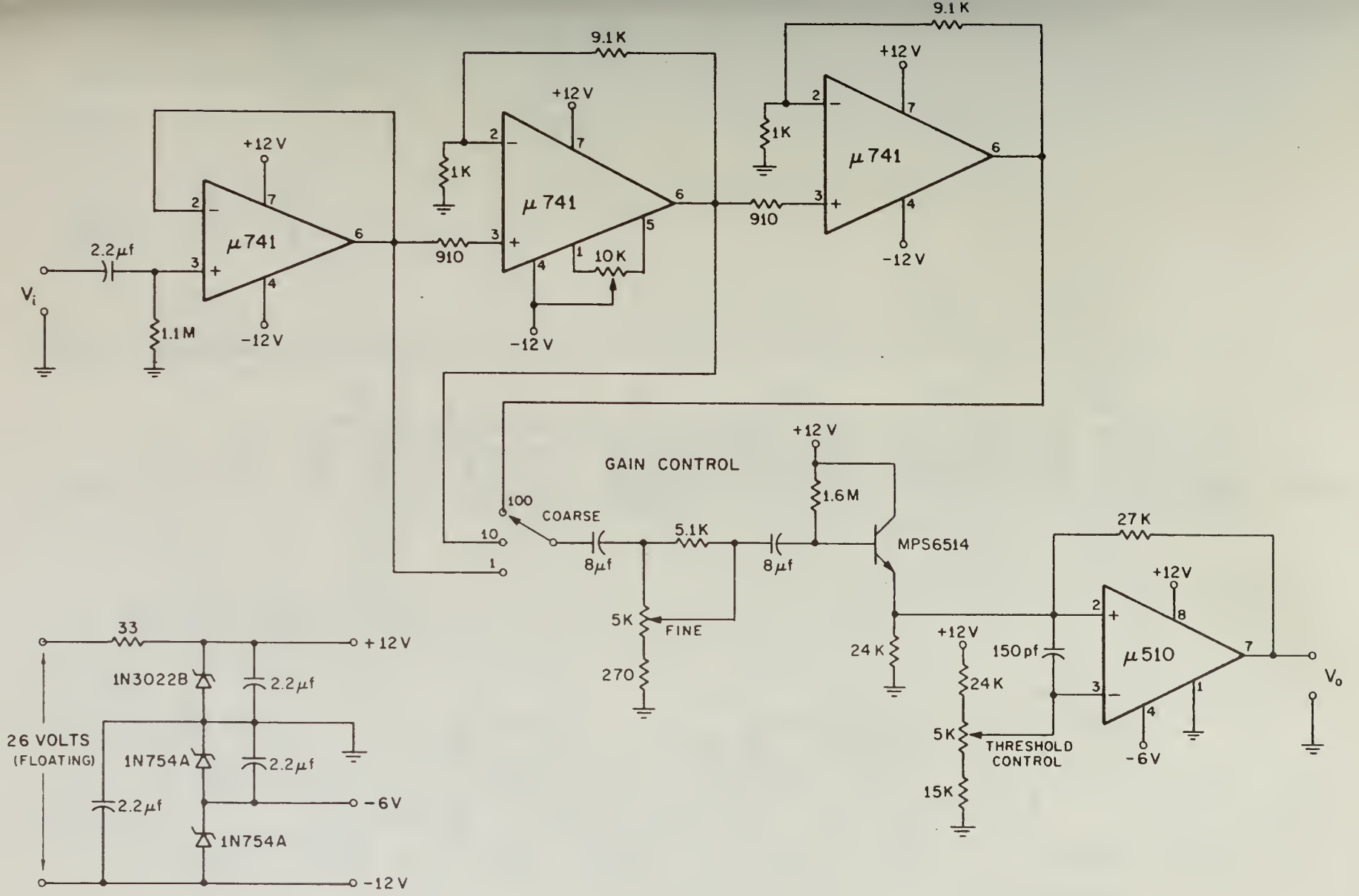

Figure A-2. Circuit Diagram of the Input Stages of the Stochastic Meter

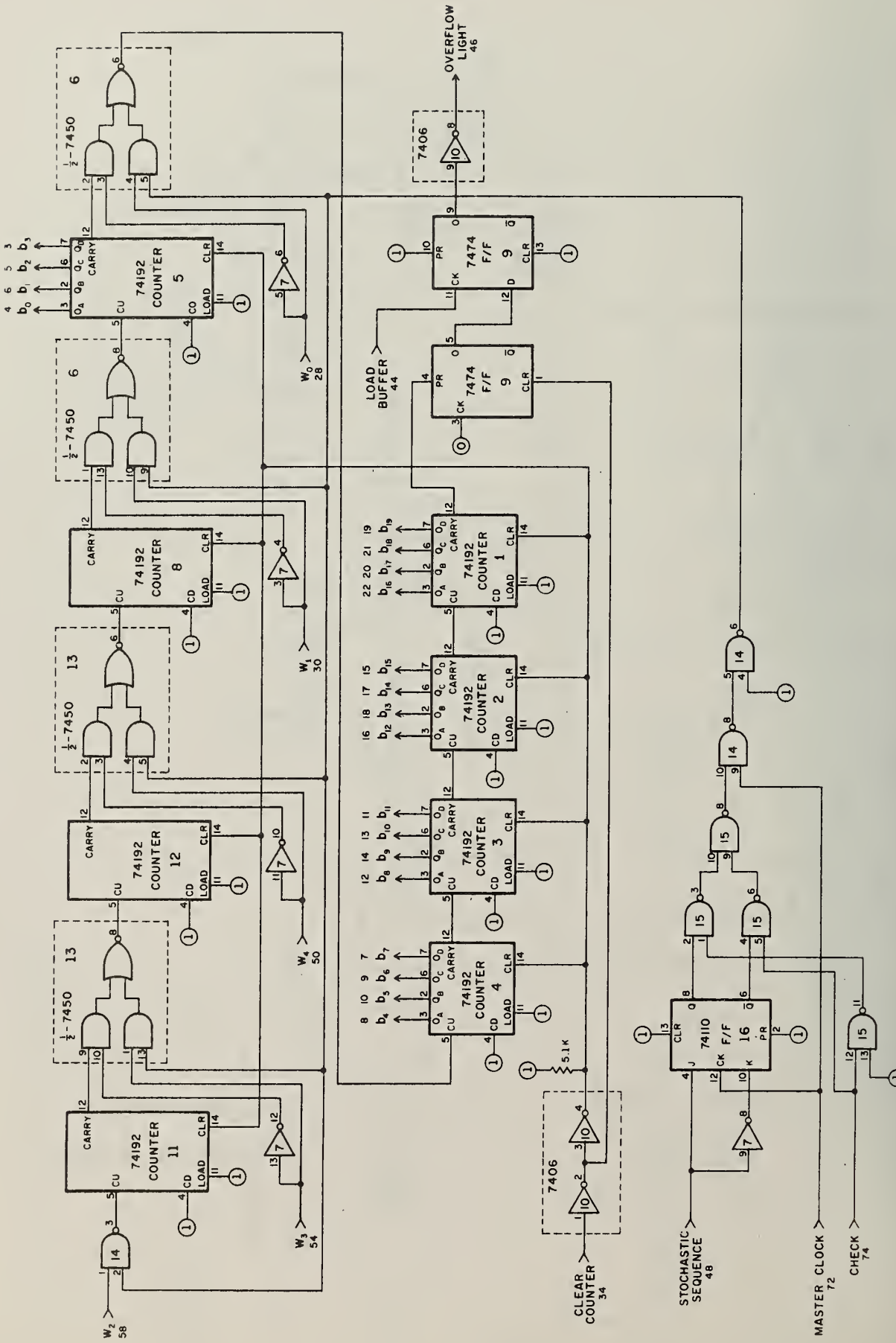

Figure A-3. Circuit Diagram of the Counter Card of the Stochastic Meter

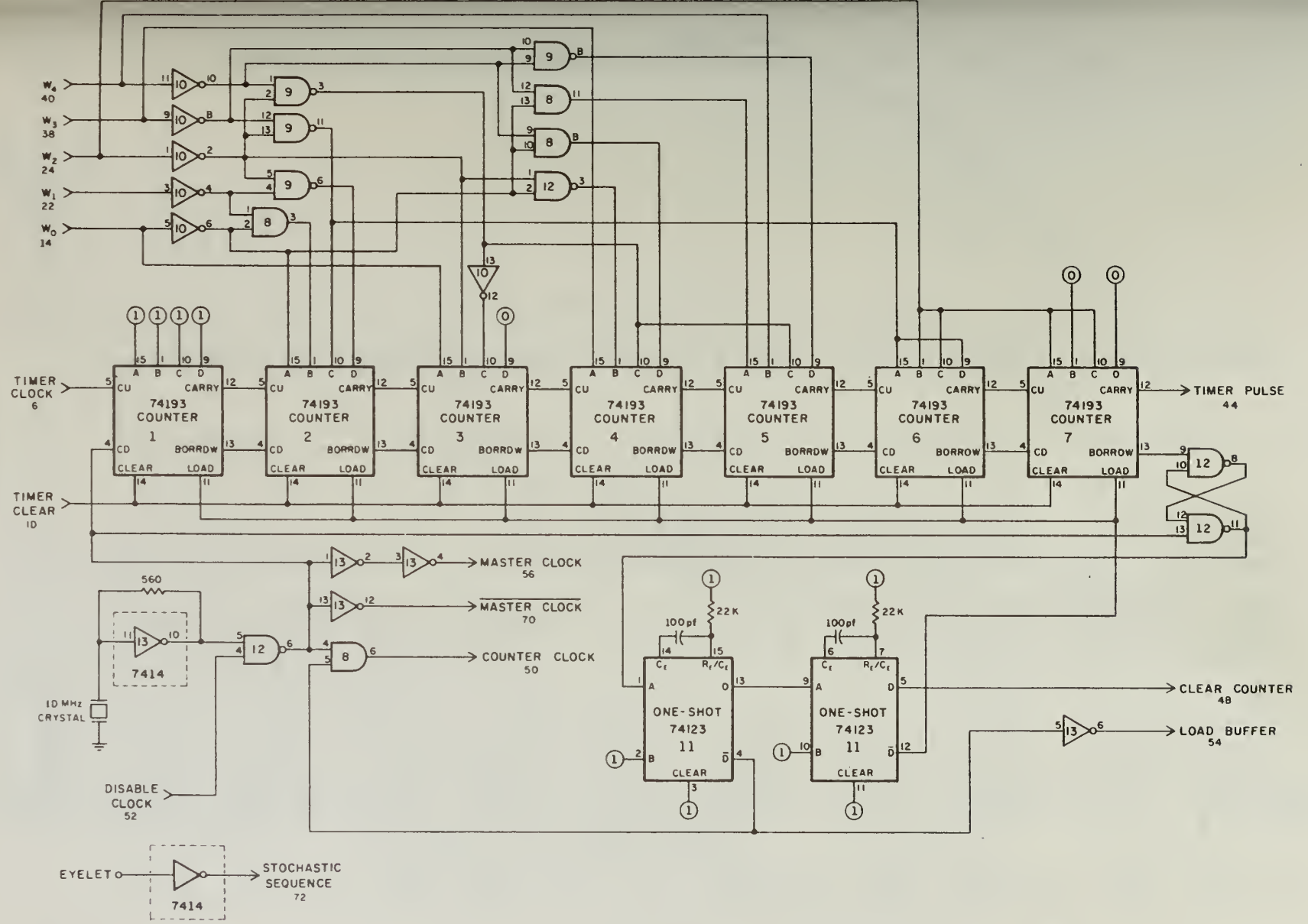

Figure A-4. Circuit Diagram of the Timer Card of the Stochastic Meter

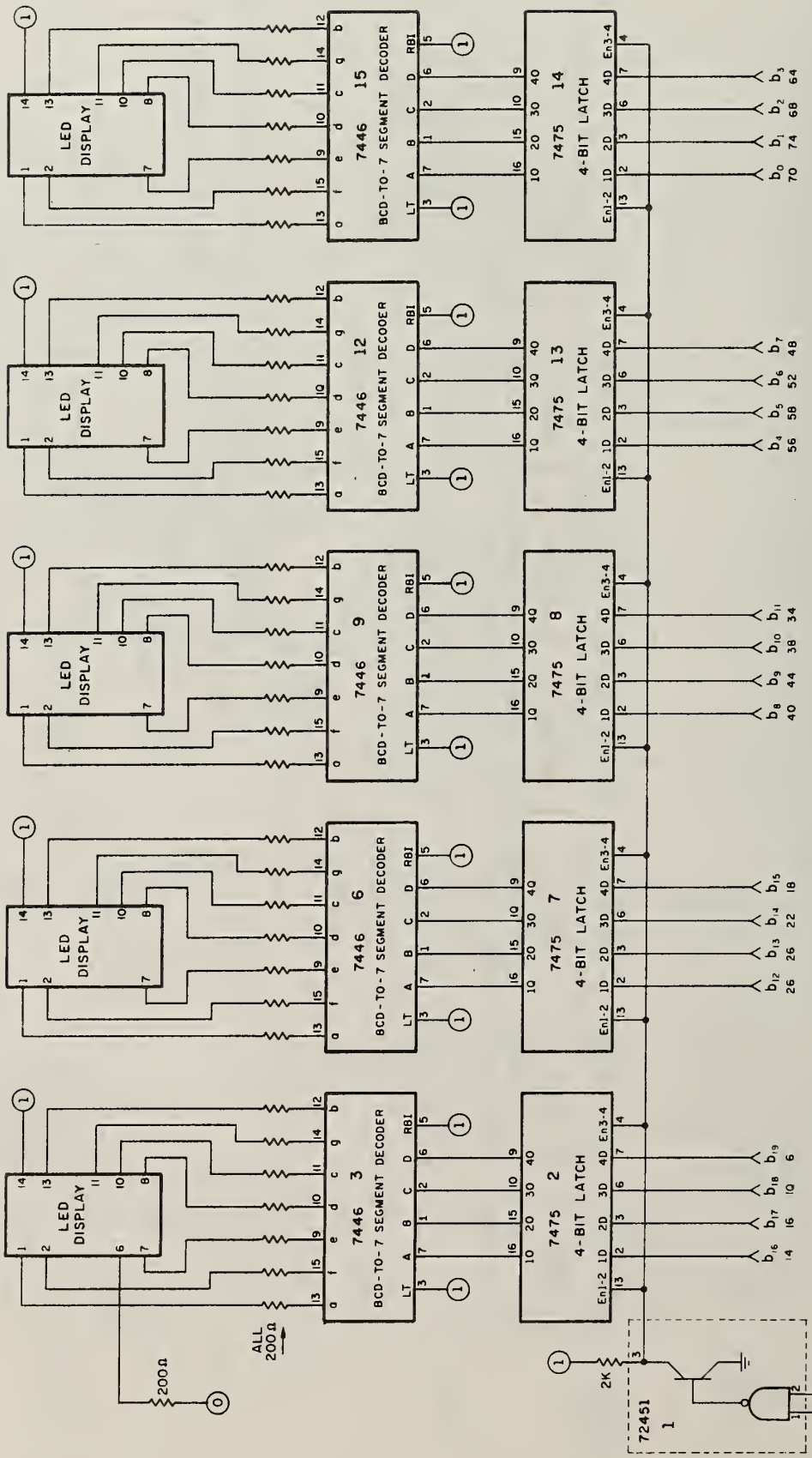

Figure A-5. Circuit Diagram of the Display Card of the Stochastic Meter

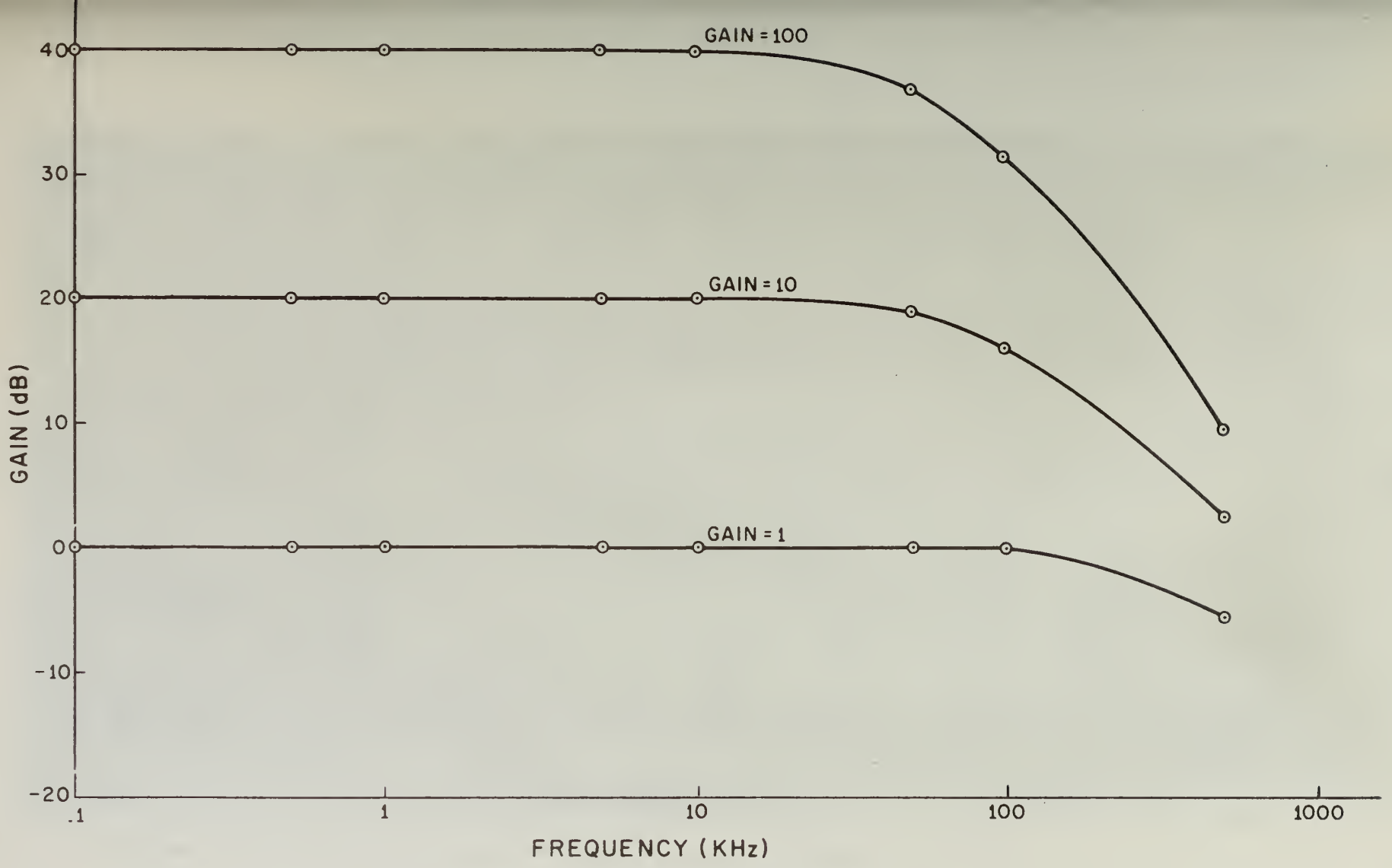

Figure A-6. Frequency Response of the Amplifier in the Stochastic Meter

TABLE A-1 Accuracy of the Stochastic Meter

a) Constant input frequency (10 KHz) and varying threshold control.

Time Average

	0.1	0.2	0.3	0.4	0.5	0.6	0.7	0.8	0.9
Standard Deviation at v_i = 100 mv.		.00020	.00042	.00017	.00025	.00031	.00019	.00066	
Standard Deviation at v_i = 200 mv.	.00058	.00034	.00014	.00017	.00017	.00014	.00013	.00023	.00043

b) Constant threshold control and varying input frequency (v_i = 200 mv.)

Frequency (KHz)

	1	5	10	20	50	100
Time Average	.39721	.40602	.40636	.40108	.37827	.31414
Standard Deviation	.00018	.00020	.00014	.00006	.00011	.00015

Note: The gain control on the stochastic meter was set--Course = 10 and Fine = 1.0--and the time period was 1 second in both of the above cases.

Figure A-7. Photograph of the Front Panel of the Stochastic Meter

APPENDIX B

Circuit Diagrams of the Tranducers

Figures B-1 and B-2 show the circuit diagrams of the temperature and luminance transducers. The 300Ω resistor used as the thermal noise source of the thermal noise temperature transducer is a 10% carbon resistor. The SM5354 transistor in the shot noise temperature transducer has similar specifications to the 2N3546 transistor. Most transistors exhibit similar shot noise to the SM5354 when the collector-to-bases junction is in the break-down region. The SM5354 transistor was chosen because the break-down voltage for the collector-to-base junction is low (~ 28 volts).

The shot noise that exists at the break-down region for the collector-to-base junction has several interesting properties. First, the amplitude of the shot noise depends upon the voltage across the junction. As the voltage across the junction increases, the amplitude of the noise first increases to a maximum and then decreases. Second, in some devices this variation occurs twice over the voltage range. Lastly, the shot noise present in the other junctions is minimal.

The FPT100 photo-transistor can be replaced by any other photo-transistor or photo-diode or photo-resistor. The selection of a different photo-sensor would change the graphs in Figures 5.3 and 5.4 but not the general nature of the shapes. The 1K resistor in parallel with the photo-transistor is needed to prevent the amplifier from oscillating.

For the flow transducer, the pressure transducer that was selected was a National LX1610GF which measures 0-60 psi gage pressure and is fluid filled.

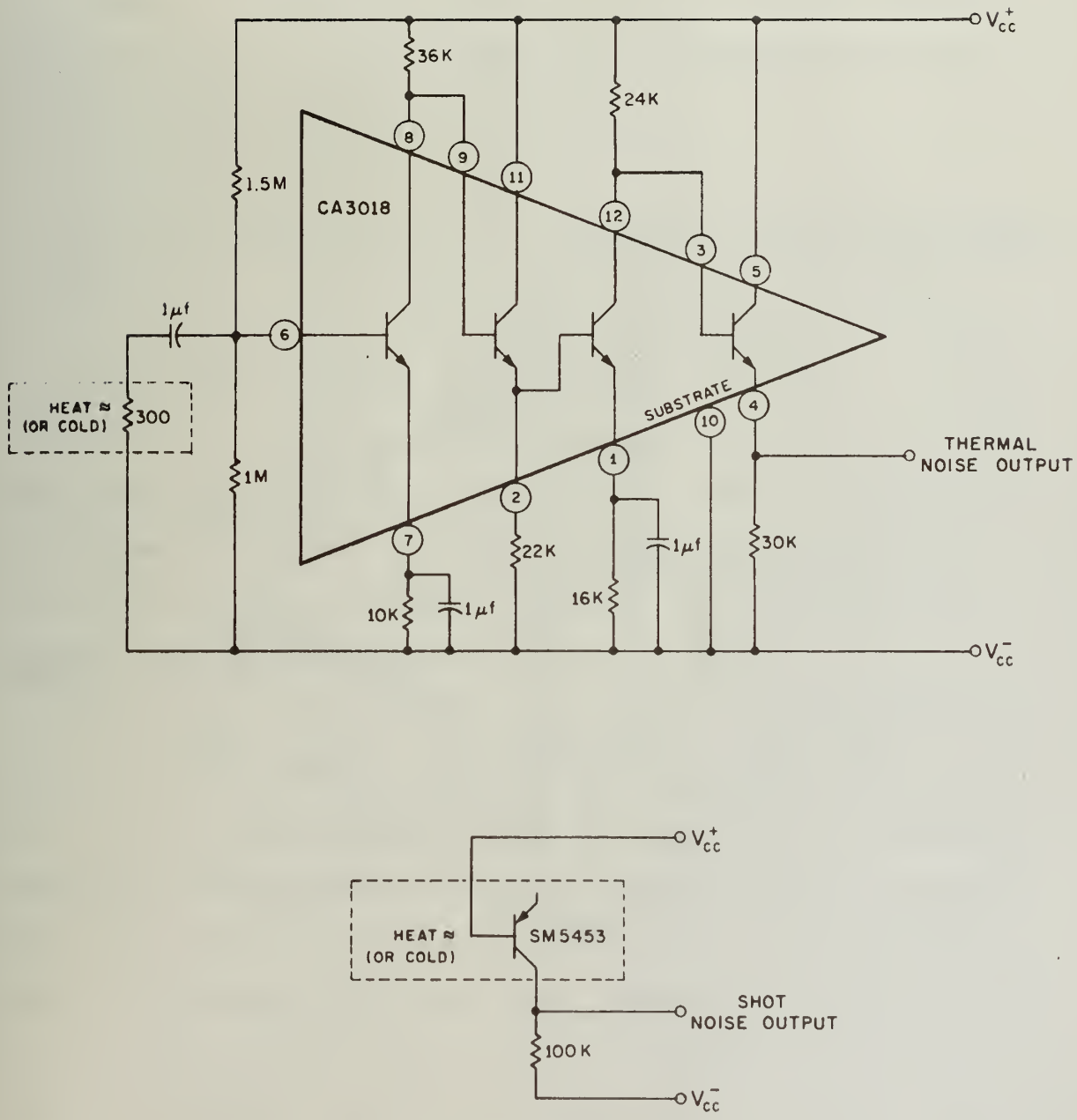

Figure B-1. Circuit Diagrams of the Thermal Noise Temperature Transducer and the Shot Noise Temperature Transducer

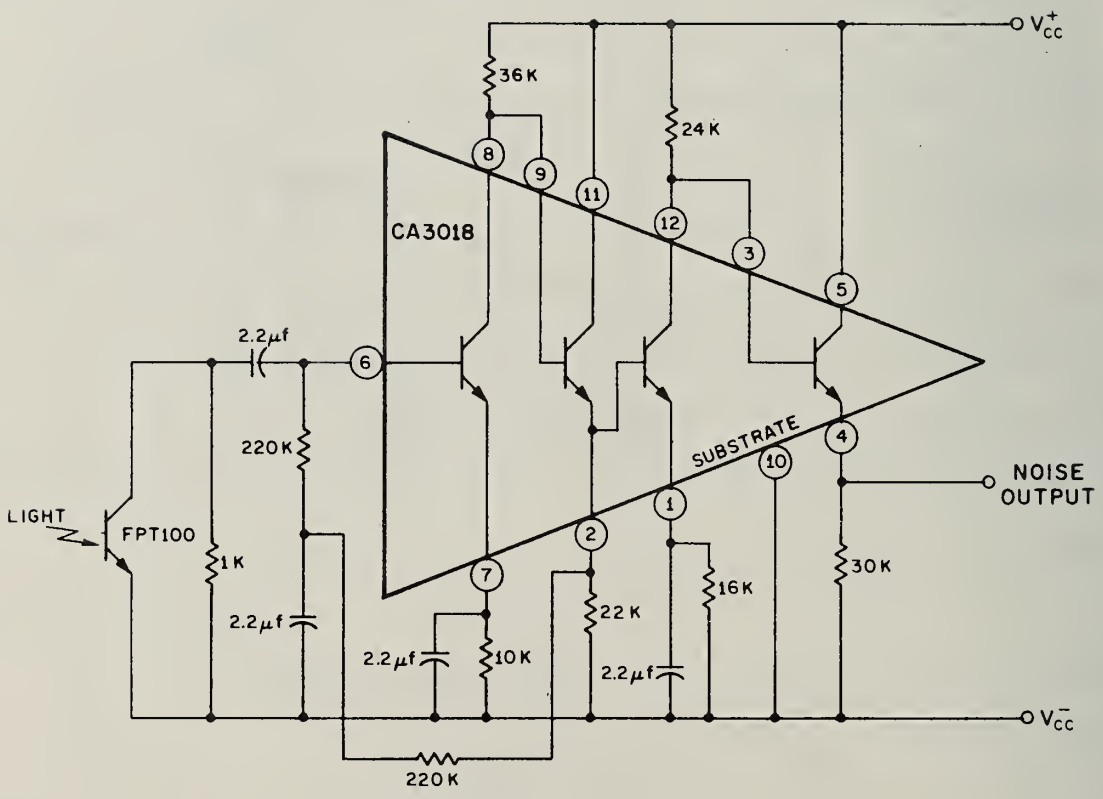

Figure B-2. Circuit Diagram of the Luminance Transducer

APPENDIX C

Experimental Procedures for Measurements with the Transducers

Tables C-1 through C-5 show the data that were used to obtain the graphs in section 5.3. The means and standard deviations are calculated by formulas similar to those given in Appendix A:

$$\text{Mean} = \frac{1}{n} \sum_{i=1}^{n} S_i \qquad \text{where } S_i = \text{samples (time averages)}$$

$$\text{and } n = \text{number of samples}$$

$$\text{and standard deviation} = \sqrt{\frac{n}{n-1} \left[\frac{1}{n} \sum_{i=1}^{n} S_i^2 - (\text{mean})^2\right]}$$

These formulas are obtained by assuming that the samples are independent and identically distributed and are found in many texts on statistics. A time period of 1 second was used to collect the data except for the flow transducer case where a 10 second time period was used.

For Tables C-1 through C-3, the temperature transducers were placed inside an oven (Associated Testing Laboratories) and the measuring device was a mercury-filled thermometer (20-110°C). A temperature setting would be made and a waiting period of at least 5 minutes would allow the environment and the contents of the oven to reach the same temperature. The samples (time averages) would then be read consecutively. Since the heating elements added spikes (and thus, noise to the transducers) to the power line when the oven turned on and off, the readings during turn-on and turn-off times of the oven were eliminated. Note that the readings for the thermal noise temperature transducer in Table C-1 at the temperature of 65°C have an unusually high standard deviation. It is suspected that several of the readings are faulty because of the above reason. The stochastic meter had

TABLE C-1. Data from the Thermal Noise Temperature Transducer

Trial	Temperature (°C)												
	25	30	35	40	45	50	55	60	65	70	75	80	85
	.23050	.20442	.21649	.19618	.17692	.17074	.14906	.13068	.13254	.12344	.11556	.08532	.07400
	.22822	.20803	.20596	.19609	.17531	.16254	.16260	.13206	.12612	.11718	.10777	.09481	.07353
	.22899	.21408	.20001	.19820	.16652	.17847	.16059	.13362	.12434	.11814	.09810	.09058	.06269
	.22628	.20734	.19876	.20151	.16473	.16372	.16485	.14005	.13325	.11638	.11004	.08738	.06519
5	.22148	.20919	.20560	.18601	.17493	.16817	.16489	.13358	.13586	.12761	.10586	.09291	.05990
	.22251	.20454	.21432	.19832	.17976	.15995	.16264	.14099	.14675	.11493	.11116	.08949	.06300
	.21515	.20762	.20632	.19753	.17494	.17610	.16622	.12990	.11291	.12474	.09843	.08698	.06351
	.21837	.20888	.20995	.19631	.17545	.16287	.16165	.13032	.10872	.11183	.11023	.09401	.05770
	.22297	.19959	.20698	.18520	.17967	.17334	.15324	.12994	.11566	.11703	.10468	.08839	.06449
10	.22181	.21080	.21364	.20176	.18038	.16296	.16517	.12626	.11450	.11822	.11156	.09018	.06677
	.22116	.19908	.20911	.19112	.18500	.16728	.15277	.12957	.11765	.12124	.10712	.08553	.06088
	.21838	.21387	.18912	.18458	.18920	.17215	.15964	.12349	.11988	.11270	.10666	.09280	.06137
	.22669	.20077	.20589	.20323	.18452	.15759	.15881	.13363	.12648	.11398	.10737	.09499	.05894
	.22593	.22040	.21022	.20071	.18153	.16439	.15707	.12884	.12783	.11894	.09374	.09280	.06345
15	.22877	.21137	.21402	.19421	.17997	.16674	.15217	.12917	.12794	.11237	.09423	.08269	.06205
	.21981	.20423	.19425	.19164	.17032	.16140	.15124	.12527	.12542	.11099	.10320	.08494	.05905
	.22107	.21035	.20380	.19772	.17787	.16680	.15660	.12282	.15135	.11405	.10107	.08883	.05863
	.22198	.20575	.21104	.19715	.17015	.17238	.16011	.13065	.18252	.11578	.09381	.08209	.05828
	.22893	.20351	.19973	.19872	.16744	.16413	.14177	.12388	.15446	.11534	.09494	.08291	.06069
20	.22624	.19711	.19394	.19383	.17325	.16919	.14503	.13320	.15352	.11094	.09789	.07798	.05802
Mean	.22376	.20707	.20546	.19551	.17639	.16705	.15728	.13040	.13189	.11679	.10368	.08824	.06261
Standard Deviation	.00427	.00572	.00750	.00541	.00645	.00552	.00697	.00483	.01801	.00461	.00672	.00485	.00459

TABLE C-2. Data from the Shot Noise Temperature Transducer

	Temperature (°C)											
Trial	30	35	40	45	50	55	60	65	70	75	80	85
	.62902	.65508	.67726	.71096	.73737	.76731	.80642	.83616	.87581	.91584	.94440	.96940
	.62954	.65383	.67683	.71095	.73596	.76746	.80644	.83476	.87598	.91574	.94437	.96920
	.62986	.65399	.67900	.70987	.73668	.76587	.80570	.83211	.87516	.91392	.94638	.96843
	.62814	.65351	.56540	.71014	.73743	.76452	.80689	.83268	.87579	.91414	.94581	.96867
5	.62899	.65295	.67794	.70974	.73697	.76573	.80651	.83279	.87564	.91498	.94591	.96770
	.62926	.65339	.67889	.70877	.73638	.76595	.80738	.83429	.87456	.91364	.94581	.96925
	.62952	.65430	.67928	.70991	.73521	.76613	.80845	.83352	.87406	.91345	.94554	.96853
	.62890	.65393	.67916	.70808	.73593	.76583	.80843	.83473	.87489	.91354	.94409	.96947
	.62880	.65279	.67905	.70981	.73438	.76595	.80602	.83364	.87247	.91442	.94419	.96993
10	.62646	.65202	.67972	.70941	.73711	.76418	.80778	.83334	.87278	.91526	.94436	.97055
	.62753	.65139	.68277	.70846	.73525	.76383	.80809	.83363	.87280	.91803	.94453	.97032
	.62667	.65175	.68038	.70989	.73634	.76403	.80639	.83500	.87304	.91526	.94483	.97049
	.62811	.65173	.68129	.70996	.73362	.76566	.80722	.83462	.87451	.91335	.94452	.96989
	.62943	.65263	.68029	.70946	.73439	.76663	.80516	.83500	.87521	.91176	.94386	.96941
15	.62986	.65219	.68004	.70958	.73551	.76561	.80555	.83456	.87361	.91233	.94486	.97013
	.62898	.65063	.67937	.70714	.73730	.76560	.80535	.83233	.87275	.91398	.94410	.97010
	.62924	.65197	.68068	.70776	.73952	.76626	.80583	.83339	.87109	.91401	.94519	.97171
	.62952	.65136	.68173	.70930	.73719	.76598	.80395	.83227	.87247	.91329	.94518	.97161
	.62937	.65116	.68046	.70856	.73698	.76496	.80376	.83185	.87182	.91170	.94508	.97191
20	.62835	.65093	.68062	.70813	.73751	.76505	.80478	.83138	.87210	.91124	.94631	.97110
Mean	.62878	.65258	.68906	.70929	.73635	.76563	.80631	.83360	.87383	.91399	.94497	.96994
Standard Deviation	.00097	.00126	.00259	.00101	.00136	.00098	.00135	.00127	.00152	.00161	.00077	.00110

TABLE C-3. Data from the Shot Noise Temperature Transducer

	Temperature (°C)										
Trial	30	35	40	45	50	55	60	65	70	75	80
	.38609	.34033	.30556	.24291	.19534	.15587	.11107	.08312	.05994	.04548	.02610
	.38574	.34114	.30535	.24302	.19545	.15539	.11130	.08340	.05970	.04537	.02528
	.38569	.34122	.30523	.24267	.19391	.15435	.11064	.08336	.05915	.04499	.02459
	.38532	.34111	.30551	.24260	.19395	.15471	.11086	.08335	.05925	.04536	.02532
5	.38453	.34019	.30423	.24231	.19325	.15434	.11246	.08380	.05818	.04376	.02674
	.38338	.33996	.30546	.24254	.19345	.15459	.11186	.08368	.05910	.04387	.02573
	.38372	.33887	.30340	.24134	.19476	.15426	.11186	.08326	.05986	.04336	.02548
	.38354	.33822	.30371	.24158	.19379	.15536	.11204	.08343	.06043	.04370	.02507
	.38338	.33788	.30424	.24174	.19401	.15493	.11100	.08280	.05985	.04301	.02520
10	.38282	.33683	.30353	.24178	.19348	.15466	.11016	.08336	.06019	.04439	.02486
	.38199	.33700	.30302	.24267	.19299	.15452	.11143	.08292	.06021	.04386	.02491
	.38203	.33609	.30289	.24132	.19348	.15478	.11200	.08228	.06114	.04355	.02509
	.38225	.33655	.30231	.24166	.19374	.15386	.11109	.08212	.06026	.04338	.02528
	.38200	.33714	.30275	.24192	.19276	.15398	.11160	.08344	.05976	.04307	.02553
15	.38171	.33599	.30144	.24055	.19334	.15417	.11192	.08166	.05848	.04347	.02517
	.38038	.33963	.30190	.24128	.19386	.15324	.11202	.08182	.06028	.04262	.02498
	.38090	.33923	.30224	.24161	.19281	.15451	.11043	.08214	.05865	.04351	.02496
	.37943	.33659	.30585	.24103	.19257	.15538	.11016	.08223	.05890	.04315	.02525
	.37990	.33514	.30560	.24107	.19352	.15498	.11119	.08290	.05854	.04275	.02502
20	.37950	.33602	.30549	.24051	.19280	.15494	.11119	.08321	.05874	.04329	.02451
Mean	.38272	.33826	.30399	.24181	.19366	.15464	.11131	.08291	.05953	.04380	.02525
Standard Deviation	.00209	.00198	.00145	.00076	.00079	.00061	.00066	.00064	.00079	.00087	.00050

a gain of 10 for the shot noise temperature transducer and a gain of about 40 for the thermal noise temperature transducer.

Table C-4 gives the data from the luminance transducer. In part a). a filter (Kodak Wratten filter no. 47B) was placed in front of the luminance transducer. Figure C-1 shows the transmittance curve for this filter. The voltage of an incandescent light bulb was then varied in order to obtain the different readings. The purpose of the filter is to maintain the shape of the spectrum radiant energy distribution as the voltage of the incandescent light bulb varies. A Tektronix J16 digital photometer with a luminance probe (foot-lamberts indicator) was used as the measuring device. Both the transducer and the photometer were placed in close proximity (about 3 inches) of each other and each were approximately one foot from the light source. The voltage of the light source was then varied so that the photometer had the proper reading for the luminance. Readings from the stochastic meter were then taken.

In part b). the voltage of the light source was fixed and the distance between light source and the transducer was varied. The direction as well as the distance is important since the luminance varies with the direction. Thus, the distance between the transducer and photometer would be varied for a particular luminance reading and then the transducer would be placed in the same position as the photometer. This procedure was especially important as the distance between the photometer and the light source became smaller. In both parts, the stochastic meter has a gain of 10.

Table C-5 shows the data obtained from the flow transducer. The average velocity was obtained by measuring the times T, required to collect 1 liter of water. The average velocity, $\bar{v}$, is calculated by

$$\bar{v} = \frac{789}{T}$$

TABLE C-4. Data from the Luminance Transducer

a) Variable voltage using filter

	Luminance (foot-lamberts)										
Trial	0	0.5	1.0	2.0	5.0	7.5	10.0	15.0	20	25	30
	.25216	.21138	.19780	.18939	.16431	.14442	.12690	.11070	.09926	.08235	.07229
	.25126	.21426	.19841	.18662	.15409	.14365	.13161	.11096	.09224	.08061	.06998
	.25416	.21215	.19964	.18635	.16028	.14408	.12540	.10856	.09605	.08148	.06970
	.25209	.21015	.19799	.18349	.15655	.13656	.13128	.10922	.09555	.08804	.07248
5	.25297	.21571	.19849	.18550	.15358	.14123	.12992	.11201	.09555	.08374	.07521
	.25582	.20403	.19491	.18188	.16019	.14379	.13020	.10551	.09303	.08164	.06458
	.24938	.21053	.19194	.18493	.15978	.13904	.12980	.10422	.09757	.08007	.07228
	.25221	.20980	.19777	.18520	.16015	.13798	.13069	.11194	.09293	.07733	.07335
	.25119	.20940	.19824	.18502	.15798	.14515	.12843	.10824	.09902	.08625	.07008
10	.24961	.20899	.19628	.18484	.15658	.13975	.13132	.10994	.09337	.08241	.07457
Mean	.25209	.21064	.19715	.18532	.15835	.14156	.12958	.10812	.09546	.08239	.07145
Standard Deviation	.00194	.00317	.00224	.00197	.00325	.00306	.00206	.00325	.00256	.00306	.00306

b) Variable distance and constant voltage

	Luminance (foot-lamberts)									
Trial	500	1000	1500	2000	2500	3000	3500	4000	4500	5000
	.27721	.26662	.26314	.25555	.24199	.21788	.17390	.12792	.10425	.09051
	.27522	.26737	.26405	.25700	.24426	.21562	.17347	.12763	.10298	.08856
	.27630	.26955	.26193	.25937	.24376	.21633	.17169	.12952	.10577	.08707
	.27400	.26868	.26562	.25707	.24389	.21470	.17423	.12877	.10272	.08664
5	.27475	.26956	.26379	.25721	.24245	.21353	.17739	.12698	.10546	.08759
	.27457	.26626	.26323	.25846	.24045	.21427	.17339	.12471	.10298	.08476
	.27250	.26760	.26422	.25629	.24022	.21258	.17157	.12295	.10423	.09165
	.27234	.26840	.26400	.25707	.24128	.21298	.16917	.12413	.10651	.08799
	.27185	.26722	.26427	.25621	.24301	.21218	.16714	.12852	.10222	.08647
10	.27090	.26786	.26312	.25653	.24333	.21257	.17076	.12499	.10354	.07970
Mean	.27396	.26791	.26374	.25708	.24246	.21426	.17227	.12661	.10407	.08709
Standard Deviation	.00203	.00113	.00097	.00111	.00144	.00187	.00288	.00225	.00144	.00327

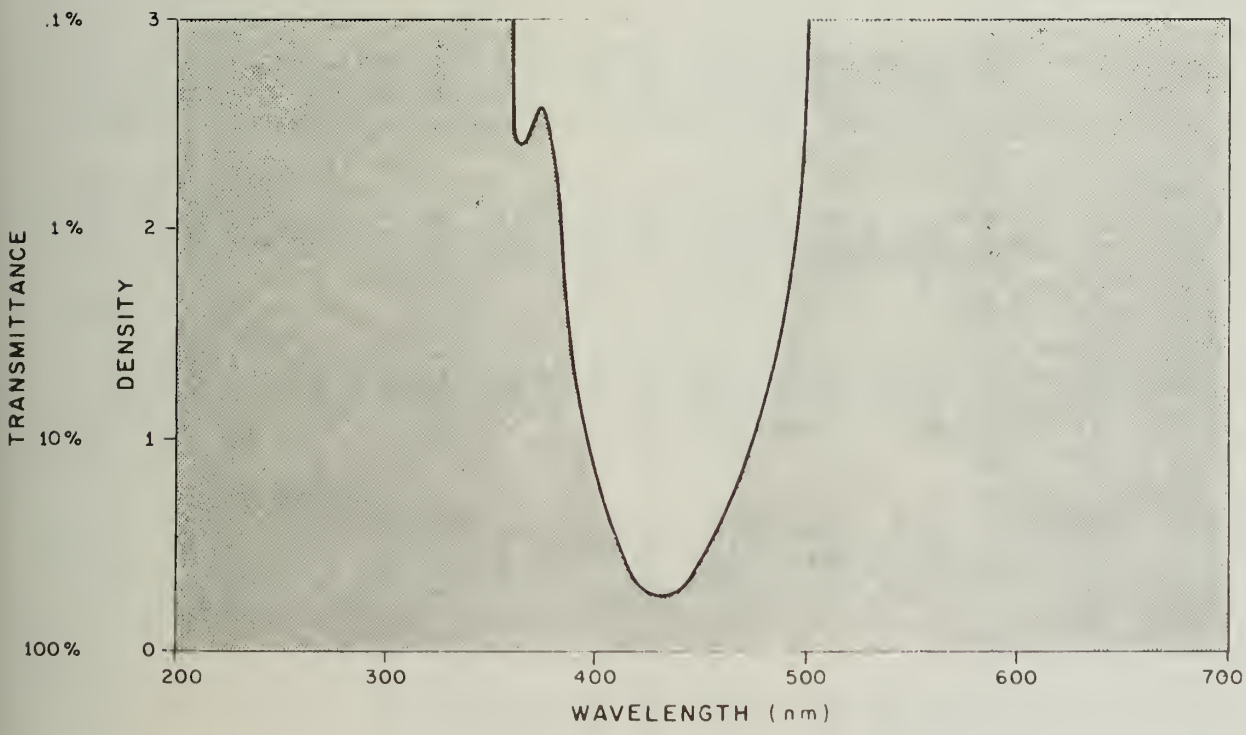

Figure C-1. Transmittance Curve for the
Kodak Wratten Filter No. 47B

TABLE C-5. Data from the Flow Transducer

	Average Velocity (cm/sec)						
Trial	75	93	120	134	171	200	243
	.0026	.0082	.0236	.0459	.0882	.1308	.1896
	.0009	.0175	.0336	.0370	.1012	.1409	.1821
	.0008	.0191	.0232	.0561	.0942	.1604	.1756
	.0004	.0135	.0246	.0497	.1095	.1538	.1739
5	.0026	.0142	.0327	.0230	.0923	.1363	.1816
	.0036	.0070	.0225	.0350	.0785	.1456	.1782
	.0009	.0119	.0279	.0324	.0887	.1541	.1812
	.0002	.0135	.0215	.0435	.1045	.1303	.1828
	.0017	.0055	.0279	.0495	.0841	.1489	.1784
10	.0019	.0082	.0140	.0556	.1153	.1337	.1801
Mean	.0016	.0119	.0252	.0428	.0957	.1435	.1804
Standard Deviation	.0011	.0045	.0057	.0107	.0117	.0107	.0043

where $\bar{v}$ is in cm/sec and T is in sec. The constant, 789, was determined by using tubes with an inside diameter of 1/2 inch. The time, T, was measured by a timer that was controlled by two level sensors--one sensor to start the timer and one to stop it. The sensors were positioned in a flask so that the volume between the two sensors was one liter. The timer was a counter with a 10 MHz clock input.

The water source was a water faucet supplied by the city water works. Because the pressure of the city water works is not constant but varies slightly, the velocity of the water through the tubes of the test set-up and the readings from the stochastic meter were affected. Thus, several data readings were ignored if the deviation from the mean appeared to be great. Also, the water faucet was such that it was difficult to set the average velocity between 100 cm/sec to 200 cm/sec. The stochastic meter had a gain of 50.

REFERENCES

1. Poppelbaum, W. J., "A Practicability Program in Stochastic Processing," proposal for the Office of Naval Research, Department of Computer Science, University of Illinois, June 1973.

2. Esch, John W., "RASCEL - A Programmable Analog Computer Based on a Regular Array of Stochastic Computing Element Logic," University of Illinois, June 1969.

3. Marvel, Orin, "Transformatrix, An Image Processor; Input and Stochastic Processor Sections," University of Illinois, April 1970.

4. Ryan, Lawrance, D., "System and Circuit Design of the Transformatrix Coefficient Processor and Output Data Channel," University of Illinois, June 1971.

5. Wo, Yiu Kwan, "Ape Machine, A Novel Stochastic Computer Based on a Set of Automonous Processing Elements," University of Illinois, February 1973.

6. Poppelbaum, W. J., Computer Hardware, Macmillan, New York, 1972.

7. Papoulis, A., Probability, Random Variables and Stochastic Processes, McGraw-Hill, New York, 1965.

8. van der Ziel, A., Noise: Sources, Characterization, Measurement, Prentice-Hall, Englewood Cliffs, N. J., 1970.

9. Feller, William, Introduction to Probability Theory and its Applications, Vol. I, John Wiley and Sons, New York, 1950.

10. Sabersky, R. H., A. J. Acosta and E. G. Hamptmann, Fluid Flow, Macmillan, New York, 1971.

11. Motchenbacher, C. D. and F. C. Fitchen, Low-Noise Electronic Design, John Wiley and Sons, New York, 1973.

12. Cramer, H. and M. R. Leadbetter, Stationary and Related Stochastic Processes, John Wiley and Sons, New York, 1967.

13. Bendat, I. S., Principles and Applications of Random Noise Theory, John Wiley and Sons, New York, 1958.

14. Goldstein, S. (ed.), Modern Developments in Fluid Dynamics, Vol. I and Vol. 2, Dover, New York, 1965.

15. van der Ziel, "Noise in Solid-State Devices and Lasers," Proceedings of the IEEE, August 1970, pp. 1178-1203.

16. Hinze, J. O., Turbulence, McGraw-Hill, New York, 1959.

17. Bhat, U. N., Elements of Applied Stochastic Processes, John Wiley and Sons, New York, 1972.

18. Parzen, Emanual, Stochastic Processes, Holden-Day, San Francisco, 1962.

19. Luxenberg, H. R. and R. L. Kuehn (eds.), Display Systems Engineering, McGraw-Hill, New York, 1968.

20. Williams, Charles S. and Orville A. Becklund, Optics, Wiley-Interscience, New York, 1972.

21. Millman, Jacob and Herbert Taub, Pulse, Digital and Switching Waveforms, McGraw-Hill, New York, 1965.

22. Wang, Shyh, Solid-State Electronics, McGraw-Hill, New York, 1966.

23. Sze, S. M., Physics of Semiconductor Devices, Wiley-Interscience, New York, 1969.

VITA

James R. Cutler was born in Mitchell, South Dakota on July 30, 1946. He attended South Dakota State University at Brookings, South Dakota and received a B.S. in Electrical Engineering in June, 1964. He then worked for the Naval Ordinance Laboratory in White Oak, Silver Springs, Maryland from July, 1968 to August, 1971. During this time, he was a participant in a graduate study program at NOL. He attended Michigan State University at East Lansing, Michigan and received his M.S. in Electrical Engineering in June, 1969.

In September, 1971 he enrolled at the University of Illinois, Urbana, Illinois. From that time, he was a research assistant working under the guidance of Professor W. J. Poppelbaum.

He is a member of the Computer Group and Solid State Circuits Group in the IEEE as well as Sigma Xi.

SECURITY CLASSIFICATION OF THIS PAGE (When Data Entered)

REPORT DOCUMENTATION PAGE

READ INSTRUCTIONS BEFORE COMPLETING FORM

1. REPORT NUMBER: UIUCDCS-R-75-723

2. GOVT ACCESSION NO.:

3. RECIPIENT'S CATALOG NUMBER:

4. TITLE (and Subtitle): MOLECULAR STOCHASTICS: A STUDY OF DIRECT PRODUCTION OF STOCHASTIC SEQUENCES FROM TRANSDUCERS

5. TYPE OF REPORT & PERIOD COVERED: Ph.D. Thesis

6. PERFORMING ORG. REPORT NUMBER:

7. AUTHOR(s): James Roland Cutler

8. CONTRACT OR GRANT NUMBER(s): N000-14-67-A-0305-0024

9. PERFORMING ORGANIZATION NAME AND ADDRESS:
Department of Computer Science
University of Illinois at Urbana-Champaign
Urbana, Illinois 61801

10. PROGRAM ELEMENT, PROJECT, TASK AREA & WORK UNIT NUMBERS:

11. CONTROLLING OFFICE NAME AND ADDRESS:
Office of Naval Research
219 South Dearborn Street
Chicago, Illinois 60604

12. REPORT DATE: April 1975

13. NUMBER OF PAGES: 87

14. MONITORING AGENCY NAME & ADDRESS(if different from Controlling Office):

15. SECURITY CLASS. (of this report):

15a. DECLASSIFICATION/DOWNGRADING SCHEDULE:

16. DISTRIBUTION STATEMENT (of this Report):

17. DISTRIBUTION STATEMENT (of the abstract entered in Block 20, if different from Report):

18. SUPPLEMENTARY NOTES:

19. KEY WORDS (Continue on reverse side if necessary and identify by block number)
Stochastic sequence
Noise source
Temperature transducer
Luminance transducer
Flow transducer
Time average

20. ABSTRACT (Continue on reverse side if necessary and identify by block number)

Molecular Stochastics is an extension of stochastic computing. The main concern of Molecular Stochastics is the generation of stochastic sequences that are used as the encoded information in stochastic computing. Also, these stochastic sequences in order to have meaning should be dependent upon some physical parameter of interest such as temperature. Thus, the problem is constructing a transducer which outputs a stochastic sequence that varies with respect to a physical parameter.

DD FORM 1 JAN 73 1473 EDITION OF 1 NOV 65 IS OBSOLETE
S/N 0102-014-6601 |

SECURITY CLASSIFICATION OF THIS PAGE (When Data Entered)

20. (Con't.)

This paper presents the necessary theory along with a discussion of a number of noise sources. These sections imply a number of transducers which were constructed and tested. The data was then compared with the result predicted by the theory.

BIBLIOGRAPHIC DATA SHEET	1. Report No. UIUCDCS-R-75-723	2.	3. Recipient's Accession No.

Title and Subtitle
MOLECULAR STOCHASTICS: A STUDY OF DIRECT PRODUCTION OF STOCHASTIC SEQUENCES FROM TRANSDUCERS

5. Report Date: April 1975
6.

Author(s)
James Roland Cutler

8. Performing Organization Rept. No. UIUCDCS-R-75-723

Performing Organization Name and Address
Department of Computer Science
University of Illinois at Urbana-Champaign
Urbana, Illinois 61801

10. Project/Task/Work Unit No.

11. Contract/Grant No. N000-14-67-A-0305-0024

Sponsoring Organization Name and Address
Office of Naval Research
219 South Dearborn Street
Chicago, Illinois 60604

13. Type of Report & Period Covered: Ph.D. Thesis

14.

Supplementary Notes

Abstracts

Molecular Stochastics is an extension of stochastic computing. The main concern of Molecular Stochastics is the generation of stochastic sequences that are used as the encoded information in stochastic computing. Also, these stochastic sequences in order to have meaning should be dependent upon some physical parameter of interest such as temperature. Thus, the problem is constructing a transducer which outputs a stochastic sequence that varies with respect to a physical parameter.

This paper presents the necessary theory along with a discussion of a number of noise sources. These sections imply a number of transducers which were constructed and tested. The data was then compared with the result predicted by the theory.

Key Words and Document Analysis. 17a. Descriptors

stochastic sequence
noise source
temperature transducer
luminance transducer
flow transducer
time average

b. Identifiers/Open-Ended Terms

c. COSATI Field/Group

Availability Statement	19. Security Class (This Report)	21. No. of Pages
Unlimited distribution	UNCLASSIFIED	87
	20. Security Class (This Page) UNCLASSIFIED	22. Price